AMPLIFIED BACKSCATTERING IN RFID COMMUNICATIONS WITH ENERGY HARVESTING TAGS

by

Denizhan Ünalan

B.S., Electrical and Electronics Engineering, Boğaziçi University, 2014

Submitted to the Institute for Graduate Studies in
Science and Engineering in partial fulfillment of
the requirements for the degree of
Master of Science

Graduate Program in Electrical and Electronics Engineering
Boğaziçi University

2018

AMPLIFIED BACKSCATTERING IN RFID COMMUNICATIONS WITH ENERGY HARVESTING TAGS

APPROVED BY:

Prof. Mutlu Koca .....
(Thesis Supervisor)

Prof. Hakan Deliç .....
(Thesis Co-supervisor)

Prof. Emin Anarım .....

Prof. Erdal Panayırcı .....

DATE OF APPROVAL: 12.10.2018

ACKNOWLEDGEMENTS

I would like to thank my supervisor Prof. Mutlu Koca and my co-supervisor Prof. Hakan Deliç for their support and guidance.

I would like to thank Prof. Emin Anarım and Prof. Erdal Panayırcı for accepting to be in the Evaluation Committee of this thesis.

I would like to thank Şenay Ünalan, Şeniz Ünalan for their support during my Master's.

I would like to thank M. Esra Yıldırım for her support during my Master's.

ABSTRACT

AMPLIFIED BACKSCATTERING IN RFID COMMUNICATIONS WITH ENERGY HARVESTING TAGS

The main objective of this thesis is to investigate the backscatter modulation-based radio-frequency identification (RFID) communication with energy harvesting tags. Thus, the study analyzes the impacts of energy harvesting on amplified backscattering and evaluates the average read probability of the RFID tags over fading channel scenarios. Two different RFID system models are constructed: the delay-constrained, which is similar to the conventional passive RFID system, and delay-tolerant, which presents a new type of an RFID system. Then a heuristic transmit power policy optimization algorithm is proposed for the backscatter modulated signals in both models in order to maximize the average read probability. By maximizing the average read probability, the optimal values of the average read probability are calculated. The optimal and simulation results are in tight agreement with each other. Thus, the tags with energy harvesting capability improve the average read probability performance of RFID communication. Furthermore, the study proves that when a chance of delay is given to the energy harvesting tag, the read probability increases significantly.

ÖZET

RFID HABERLEŞMESİNDEKİ ENERJİ HASATI YAPABİLEN ETİKETLERİN GÜÇLENDİRİLMİŞ GERİSAÇILIMI

Bu çalışmanın temel amacı gerisaçılım modülasyonu kullanan enerji hasatlama özelliğine sahip RFID etiketlerinin haberleşmesini araştırmaktır. Bu amaçla enerji hasadının güçlendirilmiş gerisaçılıma etkileri araştırıldı ve bu etiketlerin sönümlenen haberleşme kanalı durumundaki ortalama okunma olasılığı değerlendirildi.İki farklı RFID sistem modeli kuruldu. Biri geleneksel pasif RFID sistemine benzeyen gecikme kısıtı olan sistem. Diğeri ise yeni tipte gecikme toleransı olan RFID sistemi. Sonrasında iki gerisaçılım modülasyonlu model için sezgisel gönderim gücü optimizasyon algoritması önerildi. Amaç ortalama okunma olasılığını maksimuma çıkarmaktı. Ortalama okunma olasılığını maksimuma çıkararak, ortalama okunma olasılığının en iyi değerleri hesaplandı. En iyi değerler ile simülasyon değerlerinin birbirleriyle sıkı bir uyum içinde olduğu görüldü. Böylece enerji hasatlama yeteneğine sahip etiketlerin ortalama okunma olasılığını arttırdığı görüldü. Üstelik enerji hasatı yapan etiketlere, cevap verirken gecikme şansı verildiğinde, okunma olasılığının daha da arttığı görüldü.

TABLE OF CONTENTS

ACKNOWLEDGEMENTS iii
ABSTRACT iv
ÖZET v
LIST OF FIGURES viii
LIST OF SYMBOLS x
LIST OF ACRONYMS/ABBREVIATIONS xiii
1. INTRODUCTION 1
1.1. Background 1
1.2. Motivation 2
1.3. Contributions 3
1.4. Organization 4
2. FUNDAMENTALS OF RFID COMMUNICATIONS 5
2.1. An Overview of the RFID Systems 5
2.2. A Basic Circuit Representation of Far Field RFID Tags 7
2.3. Responsibilities of the Tag and the Reader 8
2.4. Types of RFID Tags 9
2.5. Performance Criteria of the RFID Systems 11
2.6. Anti-Collision Models of the RFID Systems 12
2.7. Enhanced Passive RFID Tag 15
3. SYSTEM MODEL 18
3.1. Frame Structure Model 18
3.2. Power Reflection, Large Scale Path Loss and Small Scale Fading Model 19
3.3. Energy Harvesting : Idle Time Slots 29
3.4. Backscattering Modulation : Active Time Slots 30
4. DELAY-CONSTRAINED RFID MODEL 33
4.1. Delay-Constrained Off-line Optimization 35
4.1.1. Concavity Condition of the Delay-Constrained Objective Function 36
4.1.2. Slackness Conditions of the Delay-Constrained Off-line Optimization 40

4.2. Amplification Decision Algorithm for Delay-Constrained Model 43
5. DELAY-TOLERANT RFID MODEL 46
5.1. Delay-Tolerant Off-line Optimization 47
5.2. Amplification Decision Algorithm for Delay-Tolerant Model 51
6. SIMULATION RESULTS 54
7. CONCLUSION 64
REFERENCES 65
APPENDIX A: HARVESTED ENERGY IN AN IDLE TIME SLOT 77
APPENDIX B: SIGNAL SNR IN CASE OF PASSIVE RFID TAG 79
APPENDIX C: SIGNAL SNR IN CASE OF ABEH RFID TAG 80
APPENDIX D: READ PROBABILITY UNDER RAYLEIGH CHANNEL . . 82
APPENDIX E: POWER PROFILE OF RAYLEIGH DISTRIBUTION 84
APPENDIX F: READ PROBABILITY IN DELAY-CONSTRAINED MODEL 85
APPENDIX G: READ PROBABILITY IN DELAY-TOLERANT MODEL . . 86

LIST OF FIGURES

Figure 2.1. An inductively coupled RFID system. 6

Figure 2.2. Backscatter RFID System. 7

Figure 2.3. Basic circuit representation of the far field RFID tag. 8

Figure 2.4. Reader-to-reader collision. 13

Figure 2.5. Tag-to-tag collision. 14

Figure 2.6. ABEH type RFID tag block diagram. 15

Figure 2.7. Basic circuit representation of diode-based RF energy harvester . . 16

Figure 3.1. TDMA based frame structure for a single tag. 19

Figure 4.1. Delay-Constrained RFID Model 33

Figure 4.2. Objective function and its Taylor expansion approximation 39

Figure 4.3. Amplification Decision Algorithm for Delay-Constrained RFID System 45

Figure 5.1. Delay-Tolerant RFID Model 46

Figure 5.2. Amplification Decision Algorithm for Delay-Tolerant RFID System 53

Figure 6.1. Average read probability of passive and ABEH tags versus distance between tag and reader for different energy storage sizes in delay-constrained case, together with the results in [1]. 55

Figure 6.2. Average read probability of ABEH tag versus distance between tag and reader for $E_{\max}$=1.12 μJ with the results of draw-all policy in delay-constrained case. 56

Figure 6.3. Average read probability of ABEH tag versus distance between tag and reader for different $E_{\max}$ values in delay-constrained case with their corresponding optimal values. 57

Figure 6.4. Average read probability of ABEH tag versus distance between tag and reader for $E_{\max}$=0.56 μJ and $p_{\text{int}} = 0.1$ in draw-all policy and delay-constrained and delay-tolerant cases with their corresponding upper bounds. 58

Figure 6.5. Average read probability of ABEH tag versus distance between tag and reader for $p_{\text{int}} = 0.025$ in delay-constrained and delay-tolerant cases with their corresponding optimization results. 59

Figure 6.6. Average read probability of ABEH tag versus interrogation probability for $E_{\max} = 0.56$ μJ and $d = 10$ m in delay-constrained and delay-tolerant case 60

Figure 6.7. Energy evolution of a tag with $E_{\max}$=2.24 μJ and $d = 8$ m 63

LIST OF SYMBOLS

d	Distance between the tag and the reader
d_0	Line of sight path length
d_i	i^{th} reflected path length
$E_{\text{harvest}}(t_k)$	Harvested energy without RF-to-DC inefficiency at time slot k
$E_{\max}$	Battery capacity
f_0	Carrier frequency
$f_0(.)$	Objective function of the optimization problem
$f_{\gamma_{\text{RX,reader,ABEH}}(\gamma(t_k))}$	Probability density function of the received SNR in ABEH structure at time slot k
G_{reader}	Gain of the reader antenna
G_{tag}	Gain of the tag antenna
$h_{\text{dl}}(t_k)$	Downlink flat fading Rayleigh distributed channel coefficient at time slot k
$h_{\text{ul}}(t_k)$	Uplink flat fading Rayleigh distributed channel coefficient at time slot k
I_j	j^{th} interrogation of the tag
i_ℓ	ℓ^{th} interrogation time slot
L	Total number of reflections
$\mathcal{L}$	Lagrangian of the objective function
L_{cable}	Cable loss
L_p	Path loss
M	Maximum allowed delay time slot at delay-tolerant scenario
N	Total number of the interrogations
$n_{\text{reader}}(t)$	Additive white Gaussian noise at the reader
$n_{\text{tag}}(t)$	Additive white Gaussian noise at the tag
p_{int}	Interrogation probability
$P_{\text{amp},k}$	Amplification power by the ABEH tag at time slot k
$\overline{p}_{\text{read}}$	Average read probability
$P_{\text{RX,reader}}$	Received conventional backscatter signal power by the reader

$P_{\text{RX,reader,ABEH}}(t_k)$	Received signal power caused from backscatter amplification at time slot k
$P_{\text{RX,tag}}$	Received signal power by the tag
$P_{\text{th,reader}}$	Power threshold at the reader
$P_{\text{TX,reader}}$	Transmitted signal power by the reader
$\|p'\|$	Differential reflection coefficient of the tag
q	Polarization factor
r	Reflection coefficient between the tag antenna and the chip
$\|r\|^2$	Power reflection coefficient
T_{query}	Query command time interval
T_{cw}	Continuous wave time interval
T	Time slot duration
$x(t_k)$	Transmitted CW signal from the reader at time slot k
$y(t_k)$	Received signal by the tag at time slot k
Z_{antenna}	Antenna complex impedance
Z_{chip}	Chip complex impedance
$z_{\text{enhanced}}(t_k)$	Received signal at the reader in the case of ABEH at time slot k
z_i	Normalized antenna radiation pattern of the ith wave
$z_{\text{passive}}(t_k)$	Received signal by the reader for the conventional passive RFID system at time slot k
$\varepsilon_{\text{harvest}}(t_k)$	Harvested energy with RF-to-DC inefficiency at time slot k
ϵ_r	Complex permittivity of the ground
η_{DC}	Efficiency of RF-to-DC energy conversion
η_{amp}	Efficiency of power amplifier
η_{mod}	Tag backscattering efficiency
Γ_i	Fresnel's reflection coefficient of the ith wave
$\gamma_{\text{amp},k}$	Transmitted amplification signal SNR at the ABEH tag at time slot k
$\gamma_{\text{RX,reader,ABEH}}(t_k)$	Received signal's instantaneous SNR at the reader in the ABEH structure at time slot k

$\gamma_{\text{RX,reader,passive}}(t_k)$	Received signal SNR for the conventional passive RFID system at time slot k
$\gamma_{\text{th,reader}}$	SNR threshold at the reader
$\gamma_{\text{TX,reader}}$	Transmitted signal SNR at the reader
λ	Wavelength
λ_{nj}	Multiplier of the nth constraint
σ_r^2	Variance of the AWGN at the reader
σ_{RCS}	Radar cross section of the tag
σ_t^2	Variance of the AWGN at the tag
θ_i	Incident angle of the ith wave with respect to the ground

LIST OF ACRONYMS/ABBREVIATIONS

ABEH	Amplified Backscattering via Energy Harvesting
AC	Alternating Current
AM	Amplitude Modulation
ASK	Amplitude Shift Keying
ASIC	Application Specific Integrated Circuit
AWGN	Additive White Gaussian Noise
CDMA	Code Division Multiple Access
CSI	Channel State Information
CW	Continuous Wave
DC	Direct Current
DL	Downlink
EIRP	Equivalent Isotropically Radiated Power
EM	Electromagnetic
FDMA	Frequency Division Multiple Access
FSK	Frequency Shift Keying
GSM	Global System for Mobile Communications
HF	High Frequency
IC	Integrated Circuit
ID	Identification
LC	Inductor Capacitor
LF	Low Frequency
LOS	Line of Sight
MDP	Markov Decision Process
MIMO	Multiple Input Multiple Output
NLOS	Non-line of Sight
NRZ	Non-Return to Zero
PA	Power Amplifier
PDF	Probability Distribution Function

PSK	Phase Shift Keying
RCS	Radar Cross Section
RF	Radio Frequency
RFID	Radio Frequency Identification
SC	Selection Combining
SDMA	Spatial Division Multiple Access
SNR	Signal to Noise Ratio
TDMA	Time Division Multiple Access
UHF	Ultra High Frequency
UL	Uplink
WPCN	Wireless-Powered Communication Networks

1. INTRODUCTION

1.1. Background

Wireless network systems traditionally utilize an external power source, e.g. battery, in order to energize wireless devices. Since the energy is not plentiful, energy scheduling is crucial. Although changing or charging the power source of the device prolongs the lifetime of the network devices, this may lead to environmental problems due to the nature of the batteries. In addition, it is costly to change the power source. But energy harvesting is an alternative way to increase the lifetime of the wireless network. There are multiple sources of energy, such as vibrational, photovoltaic etc. In addition, the energy of radio signals emitted by different sources is considered as a new type of energy harvesting source [2]. Harvesting the energies of ambient transmitters' radio frequency (RF) signals leads to significant interest on wireless powered networks. For example, 1μW energy can be harvested from ambient RF signals at a distance of 11 meters [3]. Since a typical wireless network includes multiple number of signal sources, the RF signals are numerous. Thus, the energy sources for harvesting procedure are unlimited compared to the traditional energy constrained batteries. As a result, the attention of many researchers has been drawn to the energy harvesting in recent years [4–7] etc.

Another energy friendly approach is backscatter communication in wireless networks. Modulated backscatter communication was first presented in [8]. In backscatter communication, the incoming signal is used as a signal source instead of generating a different signal in order to achieve communication. This approach is suitable for low-power systems because the reflected signal is the rearranged version of the received signal [9, 10]. The detailed survey about backscatter communication was introduced in [11]. In [12], the modulated backscatter system was considered in a heterogeneous environment, which means there are multiple sources of transmitters. Additionally, RF energy harvesting was also considered in [12] with hybrid receiver structure.

In hybrid backscatter communication model, the harvested energy from RF and the received signal are both the source of the backscatter modulated signal as assumed in this thesis. The wireless-powered communication networks (WPCN) were studied in [13–16] etc. The WPCN with backscatter communication was also investigated in [17], which includes ambient backscatter.

One of the important application areas of the backscatter communication is radio-frequency identification (RFID). This system is commonly used for tagging ,and its major advantage is its lower cost than those of other systems [18]. RFID systems are extensively used in such applications as transportation, non-stop toll collection, access control, source tagging, asset management, supply chain, parking, auto registration, subway entry etc [19]. In this thesis, RFID type backscatter communication with RF energy harvesting is employed.

1.2. Motivation

The relevant literature mainly focused on throughput (i.e. data rate) maximization of the WPCN [6, 15, 20–23] etc. However, the receiving signal power is another important performance measure for wireless networks. The received signal power determines the successful communication in terms of the minimum required signal threshold of the device. Thus, the receiver should reach a sufficient signal power in order to supply a healthy communication. Moreover, previous studies on data rate maximization of WPCN assume that the receiver's minimum required signal power threshold is always exceeded. While it is not true for all instances of communication in a real environment. The readability of a sensor represents the successful communication. As the name implies, the readability demonstrates the statistics or ratio of the successful communication. Therefore, the readability of the device becomes another important criterion on wireless networks, and maximization of readability has not been studied in detail except [1]. For this reason, the main motivation of this thesis is to provide research on readability of a device in WPCN.

1.3. Contributions

The main focus of this thesis is the maximization of the readability of a sensor in fading channel due to scarcity of literature on both theoretical and practical approaches of the readability phenomena. Different theoretical calculations are also given like probability distribution functions (PDF) of received signals in different cases. In addition to theoretical results and calculations, practical (i.e. heuristic) algorithm is proposed. Since another performance measure,i.e. read probability, is considered in this thesis, the system model that the thesis provides is different than the related work in the literature.

In this thesis, hybrid backscatter RFID communication with RF energy harvesting is considered in both delay-constrained and delay-tolerant scheme. The results show that the proposed heuristic algorithm is in tight agreement with corresponding optimal values. For this reason, the heuristic algorithm can be used as an optimal curve instead of implementing the optimization problem. Since the optimization problem is time-consuming algorithm, heuristic approach can be easily used to compare optimal curves (i.e. heuristic algorithm) and the future researches' results. In addition, *a priori* channel state information (CSI) requirements are reduced compared to the proposed algorithm in [1]. Additionally, the proposed algorithm is more simpler than that in [1] ,which reduces the complexity.

The delay-constrained RFID model is first presented in [1]. This model with energy harvesting improves the read range of the devices. The same model is assumed in this thesis with some changes. The updated version of the delay-constrained model in [1] also enhances the read range of a sensor. However, the delay-tolerant model is introduced as a new type of RFID system model in this thesis. Although specifications of the delay-tolerant model need to be developed, the delay-tolerant model boosts the readability of the sensor.

1.4. Organization

The organization of the thesis is as stated : In Chapter 2, the preliminary information about the RFID is described. The information provided in this chapter is necessary to construct both the delay-constrained and delay-tolerant RF energy harvesting RFID models. System model and average read probability concept are introduced in Chapter 3. The delay-constrained and delay-tolerant RFID model are presented in Chapter 4 and Chapter 5, respectively. Moreover, corresponding optimization problems and the practical heuristic power amplification algorithms are formulated in Chapter 4 and Chapter 5, respectively. Simulation results are presented in Chapter 6. The discussion of the simulation results and the contributions of this thesis to the literature are presented in Chapter 7. Future works are also exhibited. Some of the theoretical derivations are left to the Appendix A-G.

2. FUNDAMENTALS OF RFID COMMUNICATIONS

2.1. An Overview of the RFID Systems

Radio frequency identification system is a wireless communication system where the reader and the tag establish the radio link via the modulated waves. RFID is a type of barcode system with some benefits over the conventional barcode system. Some of the advantages of the RFID system are no line-of-sight requirement between the tag and the reader, working hard physical conditions like moisture, multiple tag identification etc.

There are two main different RFID tag design types in order to convey power from the reader to the tag. One is based on magnetic induction while the other one is based on electromagnetic (EM) wave capture. The electromagnetic properties of the radio frequency (RF) antenna determine their field types, which are near field and the far field, respectively [24].

The induced voltage is generated via magnetic induction in the first case [25] in low frequency (LF) or high frequency (HF) bands. The same principle is used in magnetic induction as in power transformers. Magnetically coupled RFID system is depicted in Figure 2.1. An alternating current (AC) voltage is induced at the tag because of a time-varying magnetic field that is generated at the reader. Since the tag's microprocessor requires direct current (DC) voltage, AC voltage is rectified to the DC voltage [26]. Both the antenna coils of the reader and the tag are inductor-capacitor (LC) circuits which has their own resonant frequency. A higher tune frequency means a lower number of turns in the antenna coil [24]. Tuning the right communication frequency is done with the help of this LC circuit. The main weakness of magnetic induction method is the read range. Increasing frequency of operation results in decreasing read range due to the fact that magnetic field diminishes at the factor of cube of the distance between the tag and the reader. This explains why it is called as "near field" RFID system.

The relationship between operating frequency and the induced voltage was defined in [27]. The communication between the reader and the tag is achieved via Amplitude Modulation (AM). The tag performs modulation by switching on and off its load resistor in order to send its identification (ID). This modulation of carrier signal in this type is called as "load modulation". Then the reader extracts ID information from load modulated signal coming from the tag.

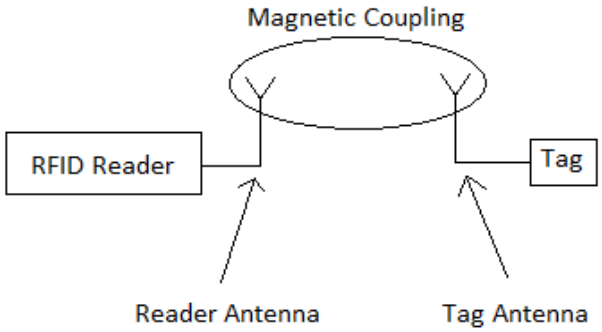

Figure 2.1. An inductively coupled RFID system.

The other RFID system is based on capturing the EM wave,i.e. electromagnetically coupled systems, which is transmitted from the reader. These systems operate in the ultra high frequency (UHF) and microwave bands. In this method, tag performs backscatter modulation [24]. A basic block diagram of the backscatter modulation or EM coupling-based RFID system is shown in Figure 2.2. The transmitted continuous EM wave from the reader contains an AC power for the tag circuitry. Voltage difference between tags' dipole antenna creates an energy for the tag microchip. Then the ID information of the tag is sent back to the reader. EM coupled systems enjoy the advantages of a higher carrier frequency. The higher the carrier frequency yields a higher electromagnetic field passing through the tag antenna, and the higher operating carrier frequency results in more voltage induced. Thus, in order to enhance read range, operating frequency should be increased if all other variables hold constant. However, this frequency approach has limitations which were defined in [27]. This class of RFID systems result in more read range with respect to the magnetically coupled RFID system.

This explains the reason of calling EM-based procedure as “far field” backscatter system. On the other hand, there is a serious problem in far field RFID systems, which does not exist in the other system. This is caused by the tags that have the same wavelength that is called as “collision problem”. The collision problems will be examined later sections in detail. A basic backscattered RFID system consists of an RF reader module or interrogator, an RF transponder or tag which has a detecting and processing unit attached to it in the form of an application specific integrated circuit (ASIC) chip [28].

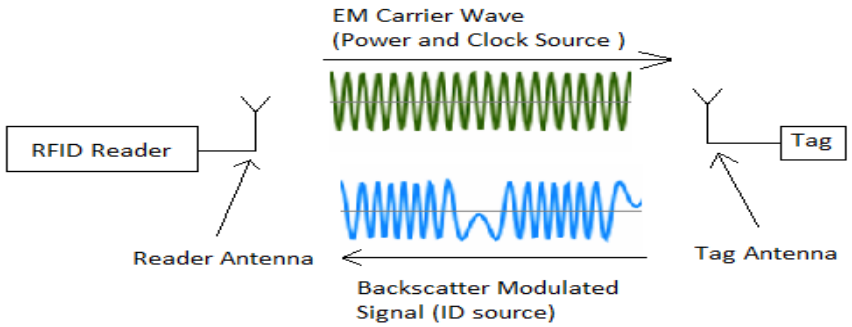

Figure 2.2. Backscatter RFID System.

2.2. A Basic Circuit Representation of Far Field RFID Tags

The tag receives the modulated signal transmitted from the reader ,which is either an active or passive tag. In a typical scenario, the reader emits a continuous radio frequency (RF) carrier sine wave [27]. Energy from the field is received by the tag when the tag gets into the RF field of the reader.

Transmitted RF signal generated by the reader induces voltage at the input terminals of the tag side. RF circuitry of the tag detects this induced voltage, and this voltage is conveyed to the capacitor so as to charge it. The basic circuit representation of the far field RFID tag [28] is shown in Figure 2.3.

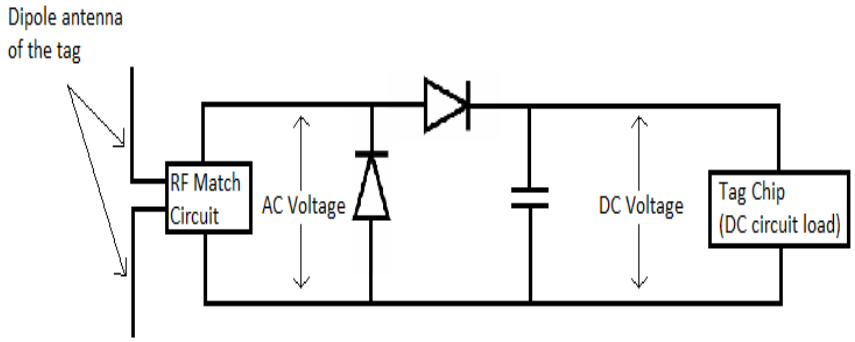

Figure 2.3. Basic circuit representation of the far field RFID tag.

The induced voltage determines the response of the transponder by considering its threshold voltage. This induced voltage is highly depends on the circuitry inside the tag and the tag transponder antenna. The incoming carrier signal by the tag is an AC signal and it needs to be converted to DC before the tag operates. A simple diode-capacitor circuit achieves this task as shown in Figure 2.3. After the tag receives sufficient energy, the processing circuit on the tag responds to the reader requests according to the protocol and the data stored on the tag. The tag modulates the carrier signal and transmits the modulated signal which is named as backscatter modulated signal. The emitted backscatter modulated RF signal, which is continuous wave (CW), from the tag is detected by the reader, and it detects and decodes this modulated signal.

2.3. Responsibilities of the Tag and the Reader

The reader supplies a carrier signal and energy to the tag and decodes the backscatter modulated signal. In [27], the energy of carrier signal generated from the reader is defined. The carrier signal is used for both as the carrier signal for return data from the tag and as a source of power to the tag. Also, the carrier signal can acts as a synchronization clock source for the tag circuitry.

The tag utilizes the energy of incoming signal, which is emitted from the reader. Then the tag resonates the reader carrier signal according to its interior capacitor and

inductor. If resonant frequency of the LC circuit matches with the incoming signal frequency and identification (ID) value transmitted from the reader matches with the tag ID, the tag circuitry activates itself. Then the tag transmits back the continuous wave signal to the reader by attaching the appropriate information.

In addition, the commonly used encoding and modulation types are also given in [27]. According to that, non-return to zero (NRZ), differential biphase and Manchester encoding are the most popular encoding types. Amplitude shift keying (ASK), frequency shift keying (FSK) and phase shift keying (PSK) are the common modulation types for generating carrier signal.

2.4. Types of RFID Tags

There are three types of RFID tags : passive, active, and semi-active or semi-passive. Although active, semi-active and passive RFID tags use RF signals emitted from the reader to communicate between the tag and the reader, they are basically different in terms of their method of powering the tags' integrated circuit (IC). An internal power source (battery) and RF communication circuitry within the tag constitute active RFID tags [26]. Internal power source continuously supplies energy to the active RFID tag in order to wake up its circuitry. These battery-powered RFID tags continuously broadcast their own signal, which are called as "beacon" signals. In order to track the tag's real time position, these beacon signals are used in high speed environments. The main limitation of the active tags is the cost of their power source. The limited lifetime is the main disadvantage of using battery in active RFID tags as opposed to the passive one. However, the power source provides a much longer read range in comparison to the semi-active and passive tags. Active tags use not only backscatter modulated signal but also a signal generated by itself, which is why the active tags have a longer read range.

Another type of RFID system is the semi-active one. Semi-active tags contain a battery which is used for running the circuitry. Therefore there is an analogy between active and semi-active tags in the manner of energy supply sources of the battery.

However, the source of communication power makes the difference between active and semi-active RFID tags. Communication between the reader and tag is achieved by using emitted wave from the reader in semi-active RFID systems as in passive RFID tags.

Passive RFID systems use tags without an initially loaded internal power source. Instead, the electromagnetic energy transmitted from an RFID reader is used to power up the passive RFID tags. The electromagnetic signal transmitted from an RFID reader, i.e. continuous wave (CW), is used in passive RFID tags to supply communication between tag and reader [26]. Thus, passive RFID system highly relies on RF energy that is transmitted from the reader in order to feed the tag with power. In other words, a passive RFID tag does not contain a battery, and its transmit signal energy is provided by the reader [29]. When a passive RFID tag meets the EM waves emitted by the reader, the coiled antenna inside the tag forms a magnetic field and induces a current in magnetically coupled RFID systems. On the other hand, the current is induced by using radio wave from the reader in backscatter RFID systems. Then the circuit of the tag is activated, which means that the tag sends its information to the reader. Since passive tags are powered remotely, they have to operate close to the reader antenna, which causes shorter read range with respect to semi-active and active ones [30]. Passive tags are inactive devices, which means that they wait for a signal coming from an RFID reader. In other words, passive tags are in the sleep mode until the reader sends an energy and a request command to the tag. Once the tag enters the reader's read zone, the energy is drawn from the RF waves, and it enters the wake mode.

Lack of battery in passive RFID tag requires stronger signals from the reader. Due to channel effect and propagation loss, strength of received signal from the tag is reduced to very low levels. In active RFID systems, the readers do not necessarily transmit their signals with a high power because they do not need to power the tag. The active RFID tag can generate high power signal back to the reader thanks to its internal battery. Another advantage of the active RFID tag is the ability of continuously powering the circuit whether the reader is close to the tag or not. In other words, the

link or the network between the tag and the reader is not necessary to wake up the tag circuitry remotely. The active RFID tags can construct communication with a reader or other tags by using beacon signals, which can be illustrated as an identification signal. Therefore, read range of the active RFID tags is much higher than the passive ones in the exchange for increased cost and high energy demand. This is the reason of why read range is important criterion for passive RFID tags. On the other hand, the main advantage of the passive tag is its cost. It has a lower price per tag compared to the active RFID tags. Therefore employing passive RFID tags is more economical for many industries.

2.5. Performance Criteria of the RFID Systems

One of the most important RFID system performance measure is the read range, which implies the maximum distance of reliable communication between the tag and the reader [31]. Tag sensitivity or tag limited regime and reader sensitivity or reader limited regime are two main factors that affects the read range [32]. Minimum required Signal to Noise Ratio (SNR), or alternatively the minimum power threshold, at the tag to run its circuitry is defined as the tag sensitivity. In addition, minimum required power level to detect the tag at the reader side is identified as the reader sensitivity.

The literature has plenty of researches on how to design an RFID reader and tag antennas and ASICs in order to improve the tag and reader sensitivity [33–40] etc. Powering the passive tag via induction is the main problem to succeed a long read range. The impacts of hardware upon the backscattered modulation is worked in [41] such as impedance mismatches. These works mainly focus on the hardware effects on RFID systems in order to enhance the system performance.

Read probability is another performance criterion of the tag in RFID systems. This measure implies the detection probability of the tag at a given distance from the reader. Therefore, it can be defined as the ratio of the number of successful read and the total number of interrogations from the reader.

2.6. Anti-Collision Models of the RFID Systems

As mentioned before, the readers initiate communication with the tags and query the tags for an appropriate information stored on them. However, this process is not performed for a single tag in a real environment. Actually, there are multiple tags in an ordinary RFID system. The reader should communicate with many of these tags in order to collect necessary information. In other words, one reader should be responsible for many of the tags in the RFID system. The readers have a finite space around them, where they can connect with the tags due to the limitations of hardware components, cost limitations and so on. This space is named as "interrogation zone" which can be thought as a coverage area of the reader [42]. The RFID collision issue can be divided into two subcategories : tag collisions and reader collisions.

The interrogation zones of the different readers may overlap that causes confusion at the management of the tags. In addition, interference from one reader to the another one is a serious problem even if their interrogation regions do not overlap. Since the frequency of the readers is the same, it may lead to inter-reader interference that is similar to the interference experienced in cellular systems. Such an interference is referred to as a "reader collision" [42]. The reader collision problems are classified as reader-to-reader collisions and reader-to-tag collisions. The reader-to-reader collision occurs when a single tag is interrogated by multiple readers at the same time, which is illustrated in Figure 2.4. In this situation, the tag might be unable to respond to any reader at all. Therefore when designing the RFID system, one should bear in mind to minimize the number and rate of reader collisions. Although the problems of reader collision are similar to the cellular telephone networks, they have some different difficulties such as tag interferences which are well defined in [42].

The primary aim of solving the reader collision problem is frequency or time, or code, or spatial allocation as in cellular networks. The resource allocation issues in the manner of cellular network concept are well studied in [43–45] etc. However, the tags in RFID system are not as smart as the mobile devices in cellular network system. For example, expecting the capability of choosing a frequency in the band

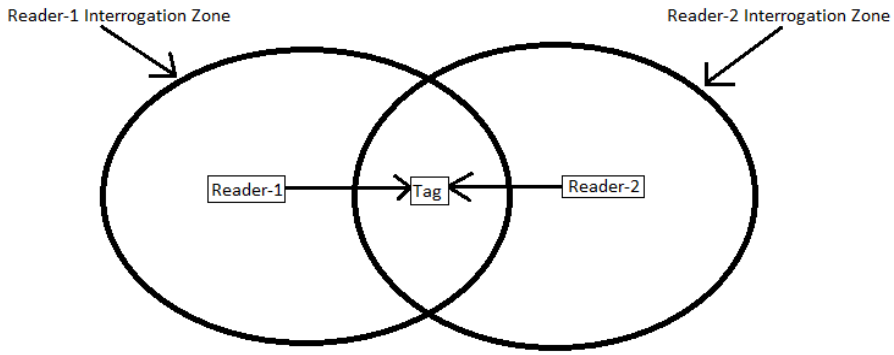

Figure 2.4. Reader-to-reader collision.

from the tag is not reasonable under the assumption of the tag is passive one. The simple solution for interference is to assign different operating time slots or different operating frequencies, or different spatial region with reuse of the same frequency. The corresponding techniques that can be used to prevent the reader collision are Time Division Multiple Access (TDMA), Frequency Division Multiple Access (FDMA), and Spatial Division Multiple Access (SDMA). Beside them Code Division Multiple Access (CDMA) is another method to prevent from the collision. The reader collision problem is studied in [46–49] etc.

The other type of collision,i.e.tag collision [26, 50, 51], becomes more important than the reader collision because the reader is typically intelligent and capable device compared to the passive tag. In practical RFID systems, tag collisions are more frequently experienced with respect to the reader collisions. Active tag collisions and passive tag collisions are the subclasses of the tag-to-tag collisions, but passive tag collision problems are more complicated than the active one because active RFID tags have an internal power source to handle the collision problem via its processing circuit. Receiving more than one tag signal at the same time, called “multi-access”, generates a confusion at the reader. This is the basic reason of the tag collision [26]. When the reader aims to communicate with the tag, the link between them may collapse because of simultaneous tag responses that is depicted in Figure 2.5

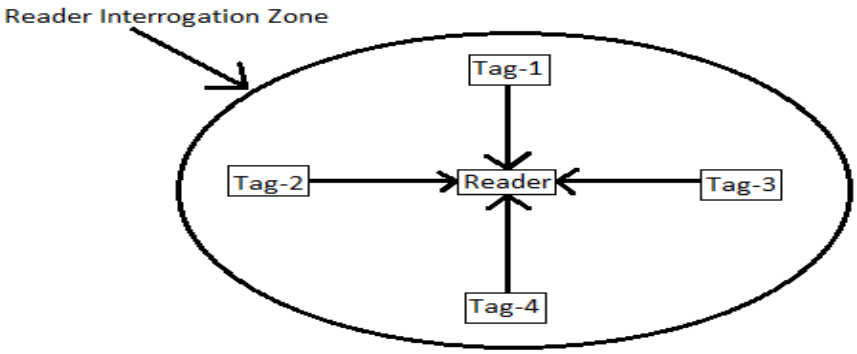

Figure 2.5. Tag-to-tag collision.

The tag collision wastes bandwidth, energy and results in identification delays. Thus it requires an anti-collision protocol at the reader side since the smarter side is the reader. The proposed solutions to the tag collision issue are the same with the ones in the reader collision, which are based on SDMA, CDMA, FDMA and TDMA [52].

SDMA-based solution relies on using multiple readers at different locations like a cell based base stations in cellular networks. By using this method, separate readers have their own coverage regions, which restrain the tag collision. The weakness of this procedure is high cost due to using multiple readers. Thus, SDMA-based solution is used rarely [52].

Allocating several transmission channels on various carrier frequencies simultaneously implies the FDMA-based solution. The major disadvantage of this procedure is the high cost for the readers because the readers should scan all the allocated channels at the same time in order to realize the tags. Therefore spectral inefficiency of this anti-collision method also makes FDMA an obsolescent solution [52].

Spreading the data over the entire spectrum via spread spectrum modulation and using pseudo random codes are the essential parts of the CDMA method, but the computations behind CDMA are so complicated for a passive tag. Another disadvantage of this procedure is to require more energy than the others [53].

TDMA-based anti-collision approaches are widely used in RFID systems because of their compatibilities. Basically, there are two different methods : tag-driven and reader-driven which are summed in [52]. The detailed explanation of proposed anti-collision procedures is associated in [53], and some of the TDMA-based anti-collision work in the literature are [54–58] etc.

2.7. Enhanced Passive RFID Tag

The new type of passive RFID tag consists of conventional passive RFID tag hardware, power amplifier (PA), energy storage device (e.g., battery or capacitor), and logic unit to determine whether strengthening of backscatter modulated signal power is performed or not [59]. Since conventional passive RFID tags have a chip inside, logic unit can be imagined as a part of that chip. This tag can be considered as a passive RFID tag because charging mechanism of this tag is supplied from the RF signal transmitted from the reader despite of the fact that it accumulates the energy. This enhanced RFID tag is defined as "amplified backscattering via energy harvesting" (ABEH) RFID tag [1], and block diagram of the ABEH RFID tag is shown in Figure 2.6.

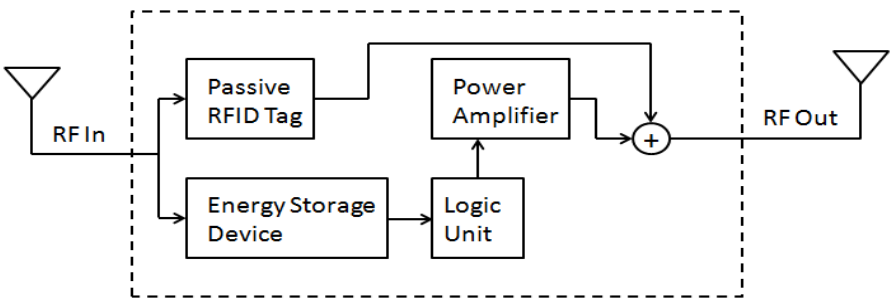

Figure 2.6. ABEH type RFID tag block diagram.

The purpose of using PA in ABEH tag is to amplify the backscatter modulated signal and of the energy storage device is to supply amplification energy to the PA by harvesting the RF signal energy during its sleep time slots [1]. In other words, energy

storage device of the tag is charged via the transmitted CW RF signal from the reader when the tag is not interrogated by the reader. Then the harvested energy is used to amplify backscatter signal when the request from the reader occurs. Therefore, ABEH type RFID tag with an empty energy storage device equals to the conventional passive RFID exactly. The logic unit decides whether the power amplification is used or not. In addition, the logic unit also determines how much amplification power will be used during backscatter modulation.

Four different energy harvesting approaches were explained in [60] with their underlying physics, hardware and the power output. These four approaches are vibrational, thermal, photovoltaic, and RF. In ABEH type RFID tag, only RF energy harvesting is considered but it can be extensible to the other ones. The basic circuit representation of diode-based RF energy harvester [61] is shown in Figure 2.7. At the first stage of this circuit, the impedance matching is performed to achieve maximum transmission line power. Then the clamping and rectifier parts are employed to convert RF signal to the DC voltage.

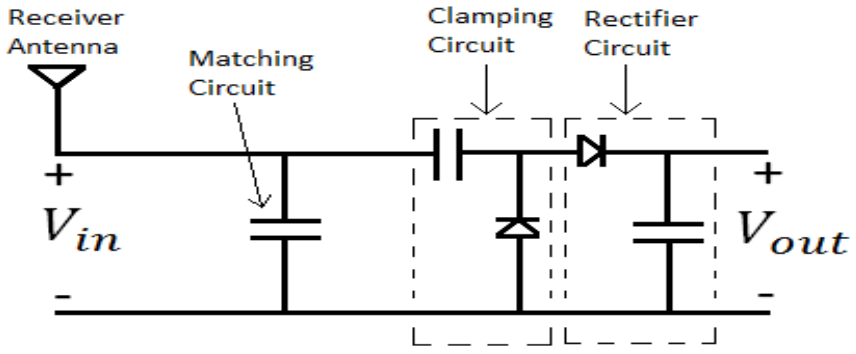

Figure 2.7. Basic circuit representation of diode-based RF energy harvester

Some of the works on RF energy harvesting in the global system for mobile communications (GSM) band were [62–64] etc. The reader limited regime or reader sensitivity was studied in [59], where the tag is designed in a similar fashion to the ABEH tag by enabling backscatter signal amplification. However, an independent

power source supplies energy to the PA, which makes the tag an active tag because initially charged power source is not allowed in the definition of the passive RFID tags. In [65], the tag sensitivity was studied by attaching a battery-assisted circuit to the tag IC. Sleep and wake cycles of the RFID tag was investigated in [66] by considering the tag as an ABEH type RFID tag. In [67], transmission policies optimization in wireless sensor networks was investigated in a way of Markov Decision Process (MDP) by employing energy harvesting. Hardware capability of the energy harvesting from RF signal emitted by the reader in RFID tag was addressed in [68]. Different energy storage approaches for RF energy harvesting were investigated in [69], where the tag is considered as an enhanced RFID tag. MDP based optimization of read range and read probability of the ABEH type RFID tag were studied in [1].

3. SYSTEM MODEL

3.1. Frame Structure Model

In this thesis, the system is considered as far-field RFID system with a single-reader and multiple-tags [26, 70]. The operation of the RFID network can be summarized with the following procedures as in Gen-2 standard [70]. A CW is transmitted from the reader to energize all the tags [66]. In order to activate the circuit of the tag, energy from the CW should be harvested. After the tags activate their circuitries, the reader starts transmitting selection signals, which are composed of "query" command and CW [1]. The tag transmits its backscatter modulated signal to the reader if it is requested with query command from the reader. This process is an "active time slot" of the RFID system for a selected tag. On the other hand, if the reader doesn't send a selection signal to the tag, then it is called as "idle time slot" [1]. The transmitted frame from the reader consists of query command,i.e. information request command from the reader, and CW period with time intervals T_{query} and T_{cw}, respectively. At the tag side, tag evaluates the incoming query command, and if the tag is requested then it performs backscatter modulation during corresponding CW period, i.e. T_{cw}. Thus, the total duration of each slot is

$$T = T_{\text{query}} + T_{\text{cw}} \quad . \tag{3.1}$$

Frame structure is based on TDMA type tag-to-reader anti-collision model, which is illustrated in Figure 3.1.

The reader generally reaches multiple tags simultaneously in a real environment, which generates a collision problem. In this thesis, one single tag is selected in each time slot with duration T so as to simplify the problem and concentrate on energy management policy of the ABEH tag as in [1]. Thus, considering only one tag for the simulations is sufficient because of the independent queries, unique identifiers of the tags, and well defined collision free model in [70] for RFID systems.

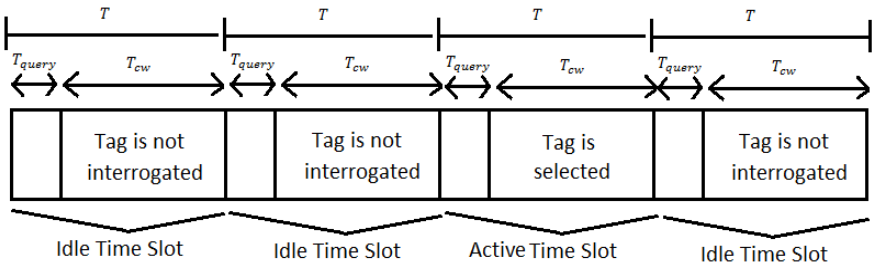

Figure 3.1. TDMA based frame structure for a single tag.

Due to the anti-collision model and independent interrogations assumptions as in [1], a simple single-reader single-tag model is sufficient to analyze energy management policy of the tag. In other words, it is assumed that the reader transmits frames continuously, which consists of query and CW subframes, and the single tag responds the reader when it is requested under these assumptions. Therefore, the behavior of the tag is divided into two different approaches as in [1]: "active time slot" and "idle time slot". Before explaining these two states, other important RFID system specifications that should be taken into account are described.

3.2. Power Reflection, Large Scale Path Loss and Small Scale Fading Model

A typical far-field RFID transponder is formed by an antenna and a chip [28]. Due to the hardware characteristics, the chip and the antenna have its own input impedances, which are complex valued. Thus, the complex input impedance of the tag antenna at the operating frequency must be directly matched to the input impedance of the chip in order to achieve maximum signal quality at the tag. One way of overcoming impedance matching problem is to use external impedance matching circuit. However, it usually increases the cost of the RFID tag. Another method is the Smith chart based impedance matching, which is performed before the tag is produced [71]. The Smith chart based impedance matching is generally used to calculate a lossless transmission line between two complex impedances [72].

In [73], power reflection coefficient of the lossless transmission line is presented by considering the conventional Smith chart, and both generator and load complex impedances. Therefore, the reflection coefficient is expressed as

$$r = \frac{Z_{\text{chip}} - Z^*_{\text{antenna}}}{Z_{\text{chip}} + Z_{\text{antenna}}} \tag{3.2}$$

where Z_{chip} is the chip complex impedance, Z_{antenna} is the antenna complex impedance and r is the reflection coefficient between the tag antenna and the chip. Thus the power reflection coefficient $|r|^2$ is

$$|r|^2 = \left| \frac{Z_{\text{chip}} - Z^*_{\text{antenna}}}{Z_{\text{chip}} + Z_{\text{antenna}}} \right|^2 . \tag{3.3}$$

The power reflection coefficient implies what fraction of the reader's transmit power is conveyed to the tag in tag-reader communication. In addition, completely matched impedances ($Z_{\text{chip}} = Z^*_{\text{antenna}}$) must yield $|r|^2 = 0$ and complete mismatch case must result in $|r|^2 = 1$. Note that $0 \leq |r|^2 \leq 1$.

The impedance mismatches and cable losses have an impact on the performance of the RFID system. Because of this performance degradation, lossy signal model should be used. By considering Friis' free-space formula and the lossy signal model in [74], the received signal power at the tag is theoretically defined as

$$P_{\text{RX,tag}} = \frac{P_{\text{TX,reader}} G_{\text{reader}} G_{\text{tag}} (1 - |r|^2)}{L_{\text{cable}}} \left(\frac{\lambda}{4\pi d} \right)^2 \tag{3.4}$$

where $P_{\text{RX,tag}}$ is the received signal power by the tag, $P_{\text{TX,reader}}$ is transmitted signal power by the RFID reader, G_{reader} is the gain of the reader antenna, G_{tag} is the gain of the tag antenna, L_{cable} is the cable loss, λ is the wavelength, d is the distance between the tag receiving antenna and the reader transmit antenna, and $|r|^2$ is the power reflection coefficient defined in equation (3.3).

The effect of reflection coefficient was studied in [74], and experimental results of this power model were presented in [74]. Note that $P_{\mathrm{TX,reader}}G_{\mathrm{reader}}$ is the Equivalent Isotropically Radiated Power (EIRP) of the reader. Cable loss is also attached to the experimental results in [74]. In addition, the effects of communication frequency on RFID system were investigated in [74], and maximum read range is reached at 900 MHz in their RFID system configuration. This model includes only large-scale path loss, which is caused by the physical nature of the electromagnetic signal propagation in a medium.

The RF power density diminishes as a factor of $\frac{1}{d^2}$ in free space conditions ,i.e. without any environmental effects, where d is the distance between the reader and the tag. On the other hand, the real environment contains different objects that causes multipath situations. Because of reflections and losses, free space assumption is not generally enough to model the wireless systems in a real environment. Thus, multipath conditions are assumed in the system model in this thesis. On the other side, a physical environment could be time or situation-dependent, which makes difficult to evaluate it. Therefore, statistical approaches are used instead of implementing every instant of the environment in order to realize it. These statistical multipath models have been explained for wireless systems or mobile communications systems in [75–78] etc. Additionally, these statistical approaches in UHF band, which is the band of interest, have been studied for indoor wireless systems in [79].

Although RFID is generally a line of sight (LOS) communication system [80], multipath effects should also be considered. Thus, Rice distributed statistical fading model is used in LOS multipath case, and Rayleigh distributed statistical fading model is selected in non-line-of-sight (NLOS) multipath environment. In this thesis, only NLOS case is performed but it can be easily extended to the LOS scenario. By considering these assumptions, received signal power at the tag in equation (3.4) is extended to

$$P_{\mathrm{RX,tag}} = \frac{P_{\mathrm{TX,reader}}G_{\mathrm{reader}}G_{\mathrm{tag}}(1-|r|^2)L_p}{L_{\mathrm{cable}}} \tag{3.5}$$

where L_p is the path loss. It is modeled as the sum of several waves reflected in ground, walls or other objects in LOS scenario as in [81]. The mathematical expression of the path loss model is given by

$$L_p = -20log\left[\frac{\lambda}{4\pi d_0}e^{-jkd_0} + \sum_{i=1}^{L}\sqrt{z_i}\Gamma_i\frac{\lambda}{4\pi d_i}e^{-jkd_i}\right] \tag{3.6}$$

where d_0 is LOS path length, d_i is ith reflected path distance, L is the total number of reflections, k is the wavenumber, z_i is the normalized antenna radiation pattern of the ith wave and Γ_i is the Fresnel's reflection coefficient of the ith wave in the object. The Fresnel's reflection coefficient is defined in [82] as

$$\Gamma_i = \frac{\cos\theta_i - q\sqrt{\epsilon_r - \sin^2\theta_i}}{\cos\theta_i + q\sqrt{\epsilon_r - \sin^2\theta_i}} \tag{3.7}$$

where ϵ_r is the complex permittivity of the ground, θ_i is the incident angle of the ith wave with respect to the ground, q is a factor which depends on polarization. Horizontal polarization yields $q = 1$ and vertical polarization results in $q = 1/\epsilon_r$.

In this thesis, it is assumed that the normalized antenna radiation pattern for all reflected waves is one, i.e. $z_i = 1, \forall i$ and Fresnel's reflection coefficient for all waves equal to 1/L, i.e. $\Gamma_i = \frac{1}{L}, \forall i$. This assumption is reasonable because larger number of reflected wave gives the lower Fresnel's reflection coefficient, which implies degradation of the system performance. Another assumption of the thesis is about the path length. Since the anti-collision model is TDMA based, each reflected wave path length is assumed to be equal. In one TDMA time slot, the received signal consists of different reflected waves, which could be either destructive or constructive with different path lengths. However, duration of each time slot is also another important parameter. If the time duration of each slot is kept short and the shortest distance between the transmitter and the receiver is small, then the reflected wave path lengths must be so close to each other. This is why equal reflected wave path lengths are reasonable.

Therefore, reduced path loss model by considering LOS case and assumptions is

$$L_p = -20log\left[\frac{\lambda}{4\pi d_0}e^{-jkd_0} + \frac{\lambda}{4\pi d}e^{-jkd}\right] \tag{3.8}$$

where $d_i = d_j = d, \forall i \neq 0, j \neq 0$. Notice that first term of the brackets in the equation (3.8) disappears in NLOS case because d_0 represents the line-of-sight wave path length. In addition, path loss is given in decibels (dB) in equation (3.8) and it decays with 20 dB/decade. Since NLOS path loss model is assumed in this thesis, first term in equation (3.8) will not be used anymore but the large scale fading model can be easily extended to the LOS case by adding the first term. Accordingly, the large-scale path loss model is assumed as a free-space model for NLOS communication. On the other hand, large-scale path loss model can also be easily extended to the other large-scale fading models by changing L_p as in equation (3.6) and by selecting different antenna settings.

As mentioned before, RFID systems utilizes backscatter communication radio link between the reader and the tag. In [80,81,83], large-scale path loss of the backscattered signal was modeled as monostatic radar equation, where radar cross section (RCS) of the tag is exploited for the incoming signal to the reader from the tag. The radar cross section refers to the measure of the tag's ability to reflect the incoming RF signal from the reader in the direction of the reader. To put it differently, it is a measure of the ratio of backscatter signal power in the reader direction. Hence, it can be imagined as the reflection coefficient of the received signal's power density. RCS depends on three factors: cross section of the projection, reflectivity of the tag and directivity of the tag. Reflectivity represents the percent of the scattered signal power, and directivity is the ratio between the power scattered back in the reader's direction and the power scattered back in the all directions. As the name implies, cross section of the projection is the area in which the signal is re-radiated. RCS was defined in [81, 83] in a similar fashion.

Under the case of no polarization mismatch with the reader antenna, the RCS of a loaded antenna can be written in a linear scale as a function of the tag antenna gain.

Hence, RCS of a loaded antenna is given by

$$\sigma_{\mathrm{RCS}} = G_{\mathrm{tag}}^2 \frac{\lambda^2}{4\pi} |p'|^2 \tag{3.9}$$

where σ_{RCS} is the RCS of the tag, G_{tag} is the tag antenna gain ,and $|p'|$ is the differential reflection coefficient of the tag. By considering monostatic radar equation, the received signal power at the reader in [81] is expressed as

$$P_{\mathrm{RX,reader}} = \frac{P_{\mathrm{TX,reader}} G_{\mathrm{reader}}^2}{L_{\mathrm{cable}}} \left(\frac{\sigma_{\mathrm{RCS}}}{4\pi}\right) \left(\frac{\lambda}{4\pi}\right)^2 \left(\frac{1}{d}\right)^4 . \tag{3.10}$$

Thus, the modified received signal power at the tag is

$$P_{\mathrm{RX,reader}} = \frac{P_{\mathrm{TX,reader}} G_{\mathrm{reader}}^2 G_{\mathrm{tag}}^2}{L_{\mathrm{cable}}} \left(\frac{\lambda}{4\pi d}\right)^4 |p'|^2 . \tag{3.11}$$

Note that differential reflection coefficient, i.e. $|p'|$, involves the power reflection coefficient of the tag, i.e. 1-$|r|^2$, and all the cable losses in the system are combined in L_{cable}. In addition, equal distance assumption of the reflected waves in equation (3.8) results in equation (3.11). Accordingly, large-scale path loss model is finalized as in equation (3.11). This model can be imagined as two cascaded free-space path loss with physical imperfections. Since this model is self-explanatory , this large-scale path loss model can be readily expanded to the different large-scale fading models, which is the powerful side of this thesis.

Beside the large-scale path loss, the transmitted RF signal experiences rapid fluctuations over a short time period, which is called as small-scale fading [84]. Since the signal distortion time period is small, the effects of the large-scale path loss may be disregarded while modeling the small-scale fading. Because of this, the small-scale fading model will be developed by disregarding the large-scale one.

In the small-scale fading, two or more versions of the transmitted signal are received because of multipath propagation delays, movement of the objects and time varying nature of the physical environment [84]. These multipath waves change the amplitude and the phase of the transmitted signal depending on the bandwidth of the transmitted signal, the propagation time of the wave etc. As mentioned before, the exact implementation of the small-scale fading channels are nearly impossible due to the fact that movement of the surrounding objects may not be estimated precisely in these channels. Consequently, some statistical channel models are used in general. In other words, wireless channel between the transmitter and the receiver are modeled as an impulse response of a linear function.

Because RFID systems are narrowband systems, fading model is also based on the narrowband, which was defined in [84]. By using the central limit theorem and independent amplitude and phase distortions, in-phase and quadrature components of the received signal are approximated as jointly Gaussian random processes. Thus, the signal envelope is modeled as Rayleigh distributed. In other words, in NLOS conditions, channel fading is assumed as Rayleigh distributed. Let the transmitted signal,i.e. CW, of the reader be written as

$$x(t_k) = \sqrt{2}\cos(2\pi f_0 t) \tag{3.12}$$

where f_0 is the carrier frequency,$\sqrt{2}$ is energy normalizing factor and $kT \leq t < (k+1)T$ runs over the k-th time slot with the duration of T. Note that time slot was previously defined as $T = T_{\text{query}} + T_{\text{cw}}$. The duration of the query command is assumed to be much shorter than the duration of the CW, i.e. $T_{\text{query}} \ll T_{\text{cw}}$, which results in $T \approx T_{\text{cw}}$.

A link between transmit antenna of the reader and the receiver antenna of the tag is referred as downlink (DL), and the link between transmit antenna of the tag and the receive antenna of the reader is named as uplink (UL). During each TDMA time slot, the DL and the UL channels are assumed as frequency flat small-scale fading, which means the channel coefficient is constant over every time slot and it changes from one time slot to the another one as independent and identically distributed (i.i.d.) random

variables. Another assumption is about the RFID reader. In this thesis, bistatic RFID readers are assumed, where they use two antennas. One of these antennas is used for transmission and the other one is used for reception as in [1]. The bistatic RFID readers were defined in [31, 85]. Operating without RF isolator is the main advantage of the bistatic RFID reader because the monostatic one utilizes only one antenna for both transmission and reception as described in [86–90]. It is also presumed that the distance between the tag and the reader is the same for both DL and UL channels. Therefore, the received signal by the tag at time slot k can be expressed as

$$y(t_k) = \sqrt{P_{\mathrm{RX,tag}}} h_{\mathrm{dl}}(t_k) x(t_k) + n_{\mathrm{tag}}(t) \tag{3.13}$$

where $kT \leq t < (k+1)T$, $h_{\mathrm{dl}}(t_k)$ is the downlink flat fading Rayleigh distributed channel coefficient at time slot k, $x(t_k)$ is the transmitted signal from the reader at time slot k, and $n_{\mathrm{tag}}(t)$ is an additive white Gaussian noise (AWGN) of the tag in the band of interest with zero mean and σ_t^2 variance, i.e. $n_{\mathrm{tag}}(t) \sim \mathcal{N}(0, \sigma_t^2)$.

In a typical conventional passive RFID system, the incoming signal from the reader is re-radiated by the tag to the reader as mentioned before. Multiple-input multiple-output(MIMO) conventional passive RFID backscattering channel models were studied in [91–94] etc. Additionally, their corresponding two way statistical channel model was well defined in [95]. Measurements in [85, 96] showed that the conventional passive RFID could be modeled as a cascaded DL and UL channel by considering both path loss and small-scale fading. Therefore, regarding the cascaded channel model, the received signal by the reader for the conventional passive RFID system is given as

$$z_{\mathrm{passive}}(t_k) = \sqrt{P_{\mathrm{RX,reader}}} h_{\mathrm{dl}}(t_k) h_{\mathrm{ul}}(t_k) x(t_k) + n_{\mathrm{reader}}(t) \tag{3.14}$$

where $kT \leq t < (k+1)T$, $P_{\mathrm{RX,reader}}$ is the received conventional backscatter signal power by the reader at time slot k. By assuming the free space communication in the

form of classical radar equation as in [31], $P_{\mathrm{RX,reader}}$ becomes

$$P_{\mathrm{RX,reader}} = P_{\mathrm{TX,reader}} G_{\mathrm{reader}}^2 G_{\mathrm{tag}}^2 \left(\frac{\lambda}{4\pi d}\right)^4 . \tag{3.15}$$

In Section 2.7, the enhanced passive RFID tag was explained, and this new type tag was named as "ABEH" RFID tag. This new tag adds some energy to the backscatter signal by using its energy storage device. For this reason, the transmitted signal from the tag involves power amplification, which is exposed to the UL fading and large-scale path loss. By considering Rayleigh distributed flat fading DL and UL channels and path loss, the envelope of the received signal at the reader can be given as

$$\begin{aligned} |z_{\mathrm{enhanced}}(t_k)| =& \sqrt{P_{\mathrm{RX,reader}} |h_{\mathrm{dl}}(t_k)|^2 + P_{\mathrm{RX,reader,ABEH}}(t_k)} |h_{\mathrm{ul}}(t_k) x(t_k)| \\ &+ |n_{\mathrm{reader}}(t)| \end{aligned} \tag{3.16}$$

where $kT \leq t < (k+1)T$, $|z_{\mathrm{enhanced}}(t_k)|$ is the envelope of the received signal at the reader in the case of power amplification, $h_{\mathrm{ul}}(t_k)$ is the uplink flat fading Rayleigh distributed channel coefficient at time slot k, $x(t_k)$ is the transmitted CW signal from the reader at time slot k, and $n_{\mathrm{reader}}(t)$ is the AWGN of the reader in the band of interest with zero mean and σ_r^2 variance, i.e. $n_{\mathrm{reader}}(t) \sim \mathcal{N}(0, \sigma_r^2)$. The first term of the sum inside the square root in equation (3.16) represents the conventional passive RFID backscatter signal while the second term represents the power amplified backscatter signal with the help of energy storage device. The received signal power caused from the backscatter amplification [1], $P_{\mathrm{RX,reader,ABEH}}$, is given by

$$P_{\mathrm{RX,reader,ABEH}}(t_k) = P_{\mathrm{amp},k} G_{\mathrm{reader}} G_{\mathrm{tag}} \left(\frac{\lambda}{4\pi d}\right)^2 \tag{3.17}$$

where $P_{\mathrm{amp},k}$ is the used amplification power by the ABEH tag at time slot k. Accordingly, the envelope of the received signal by the reader coming from the ABEH tag can

be expressed as

$$
\begin{aligned}
|z_{\text{enhanced}}(t_k)|^2 = {} & P_{\text{TX,reader}} G_{\text{reader}}^2 G_{\text{tag}}^2 \left(\frac{\lambda}{4\pi d}\right)^4 |h_{\text{dl}}(t_k)|^2 |h_{\text{ul}}(t_k)|^2 |x(t_k)|^2 \\
& + P_{\text{amp},k} G_{\text{reader}} G_{\text{tag}} \left(\frac{\lambda}{4\pi d}\right)^2 |h_{\text{ul}}(t_k)|^2 |x(t_k)|^2 \\
& + |n_{\text{reader}}(t)|^2 \quad .
\end{aligned} \tag{3.18}
$$

Notice that the imperfections caused by hardware, impedance mismatches etc. are not modeled in equation (3.18). However, the imperfections such as the impedance mismatches in equation (3.3), antenna polarizations and antenna radiation patterns in equation (3.6) , the Fresnel's reflection coefficient in equation (3.7) and other hardware effects can cause significant performance losses. Thus, these imperfections must be included in signal model in order to achieve a more realistic RFID system model. The power reflection coefficient in equation (3.3) is in the range of 0 and 1,i.e. $0 \leq |r|^2 \leq 1$. In addition, antenna polarization, Fresnel's reflection coefficient are also in the range of -1 and 1. These imperfections have a multiplicative effect on signal model. Therefore, all these imperfections are combined in one efficiency factor as in [1, 31]. Finally, the envelope of the lossy combined received signal by the reader coming from the ABEH tag can be denoted by

$$
\begin{aligned}
|z_{\text{enhanced}}(t_k)|^2 = {} & P_{\text{TX,reader}} G_{\text{reader}}^2 G_{\text{tag}}^2 \left(\frac{\lambda}{4\pi d}\right)^4 \eta_{\text{mod}} |h_{\text{dl}}(t_k)|^2 |h_{\text{ul}}(t_k)|^2 |x(t_k)|^2 \\
& + P_{\text{amp},k} G_{\text{reader}} G_{\text{tag}} \left(\frac{\lambda}{4\pi d}\right)^2 \eta_{\text{amp}} |h_{\text{ul}}(t_k)|^2 |x(t_k)|^2 \\
& + |n_{\text{reader}}(t)|^2
\end{aligned} \tag{3.19}
$$

where η_{mod} is the tag backscattering efficiency which was defined in [31], and η_{amp} is the efficiency of power amplifier (PA). η_{mod} includes impedance mismatches, antenna imperfections and etc. In addition, both inefficiency coefficients are in the range of 0 and 1, i.e. $0 \leq \eta_{\text{amp}} \leq 1$ and $0 \leq \eta_{\text{mod}} \leq 1$.

3.3. Energy Harvesting : Idle Time Slots

The RFID tag is exposed to two different time slots as mentioned in Section 3.1. One is the idle time slot and the other one is the active time slot. The RFID tag experiences idle time slots when it is not interrogated by the reader because of the TDMA-based anti-collision frame structure. Thus, the tag harvests the energy of the incoming RF signal, which is transmitted by the reader during the idle time slots. The harvested energies are utilized by the ABEH RFID tag during active time slots in order to amplify the backscatter signal. Hence, the received energy at time slot k by the ABEH tag can be derived as

$$\begin{aligned} E_{\text{harvest}}(t_k) &= \int_{t_k}^{t_{k+1}} |y(t_k)|^2 dt = \int_{t_k}^{t_{k+1}} \left| \sqrt{P_{\text{RX,tag}}} h_{\text{dl}}(t_k) x(t_k) + n_{\text{tag}}(t) \right|^2 dt \\ &= \int_{t_k}^{t_{k+1}} \left| \sqrt{P_{\text{TX,reader}} G_{\text{reader}} G_{\text{tag}} \left(\frac{\lambda}{4\pi d} \right)^2} h_{\text{dl}}(t_k) x(t_k) + n_{\text{tag}}(t) \right|^2 dt \quad . \end{aligned} \tag{3.20}$$

Since the transmitted signal from the reader, i.e. $x(t_k)$, and the AWGN of the tag, i.e. $n_{\text{tag}}(t)$, are independent, the harvested energy during each idle time slot can be calculated as

$$E_{\text{harvest}}(t_k) = T P_{\text{TX,reader}} G_{\text{reader}} G_{\text{tag}} \left(\frac{\lambda}{4\pi d} \right)^2 |h_{\text{dl}}(t_k)|^2 + T\sigma_t^2 \tag{3.21}$$

where T is the TDMA time slot duration and σ_t^2 is the variance of the AWGN of the tag. Derivation of the harvested energy in the idle time slot is explained in Appendix A. As presumed in [1], noise energy is supposed to be negligible compared to the received signal energy, i.e. $T\sigma_t^2 \ll T P_{\text{TX,reader}} G_{\text{reader}} G_{\text{tag}} (\frac{\lambda}{4\pi d})^2 |h_{\text{dl}}(t_k)|^2$. For this reason, the harvested energy in idle time slots can be approximated as

$$E_{\text{harvest}}(t_k) \approx T P_{\text{TX,reader}} G_{\text{reader}} G_{\text{tag}} \left(\frac{\lambda}{4\pi d} \right)^2 |h_{\text{dl}}(t_k)|^2 \quad . \tag{3.22}$$

On the other hand, equation (3.22) assumes perfect RF-to-DC energy conversion. In reality, any energy conversion results in some losses, which is caused by hardware, phys-

ical environment etc. In order to implement more realistic harvesting model, energy conversion efficiency must be included in the model. In [40], RF-to-DC energy conversion efficiency was explained, and used in [1] by considering RFID energy harvesting. In this thesis, RF-to-DC energy conversion is also considered. Hence, the lossy model of the harvested energy during idle time slots is given by

$$\varepsilon_{\text{harvest}}(t_k) = \eta_{\text{DC}} E_{\text{harvest}}(t_k) = \eta_{\text{DC}} T P_{\text{TX,reader}} G_{\text{reader}} G_{\text{tag}} \left(\frac{\lambda}{4\pi d}\right)^2 |h_{\text{dl}}(t_k)|^2 \qquad (3.23)$$

where η_{DC} is the efficiency of the RF-to-DC energy conversion, which is presumed to be constant over entire communication. To put it simply, it is not defined as time varying. Since it represents the efficiency, it is in the range of zero and one, i.e. $\eta_{\text{DC}} \in [0, 1]$, where $\eta_{\text{DC}} = 1$ shows that the energy conversion is performed without loss and $\eta_{\text{DC}} = 0$ implies that the energy harvesting is not realized due to the inefficiency of the RF-to-DC conversion. Conventional passive RFID systems do not have energy harvesting capability. Therefore, $\eta_{\text{DC}} = 0$ model also represents conventional passive RFID tag. One final note about energy harvesting is the capacity of the energy storage device. It is presumed that the harvested energy can not exceed the maximum value of the battery in this thesis. Suppose that the battery is of size $E_{\max}$. Then it is obvious that the harvested energy must be less than or equal to battery capacity, i.e. $\varepsilon_{\text{harvest}}(t_k) \leq E_{\max}, \forall k$.

3.4. Backscattering Modulation : Active Time Slots

Another type of the time slot is the active time slot in which the reader interrogates the RFID tag. During the active time slots, the interrogated tag transmits back the incoming query signal of the reader. This process is named as "backscatter modulation." The reflected signal includes necessary information about the tag in order to be evaluated by the reader. In other saying, the reader transmits its query signal to the tag and waits for a response from the tag during each active time slot. There are a lot of factors that have an impact upon the backscatter modulation such as tag sensitivity, reader sensitivity, CSI, imperfections in RFID system etc. In this

thesis, tag sensitivity is not considered, which means that the tag perfectly detects each transmitted signal by the reader even if the communication channel is very poor or the incoming signal's SNR is so low. On the other hand, poor channel conditions have an influence on energy harvesting and/or backscatter signal, which degrades overall RFID system performance in the terms of read probability and read range.

Firstly, the SNR of the received signal at the reader must be derived in order to measure the performance of the RFID system either the tag is assumed as conventional passive or ABEH type. In equation (3.14), the received signal by the reader in the conventional passive RFID system is given. The envelope of this signal can be given by

$$|z_{\text{passive}}(t_k)| = \left| \sqrt{P_{\text{TX,reader}} G_{\text{reader}}^2 G_{\text{tag}}^2 \left(\frac{\lambda}{4\pi d}\right)^4} h_{\text{dl}}(t_k) h_{\text{ul}}(t_k) x(t_k) + n_{\text{reader}}(t) \right| \quad . \tag{3.24}$$

In Appendix B, the SNR of the received signal by the reader is derived under the assumption of conventional passive RFID system. Accordingly, the received signal SNR is derived as

$$\gamma_{\text{RX,reader,passive}}(t_k) = \frac{P_{\text{TX,reader}} G_{\text{reader}}^2 G_{\text{tag}}^2}{\sigma_r^2} \left(\frac{\lambda}{4\pi d}\right)^4 |h_{\text{dl}}(t_k)|^2 |h_{\text{ul}}(t_k)|^2 \quad . \tag{3.25}$$

However, equation (3.25) does not contain any imperfections such as power reflection coefficient that caused by impedance mismatch. In order to realize more realistic system model, lossy model must be used. Therefore, the lossy model of the instantaneous SNR of the received signal by the reader can be given by

$$\gamma_{\text{RX,reader,passive}}(t_k) = \frac{P_{\text{TX,reader}} G_{\text{reader}}^2 G_{\text{tag}}^2}{\sigma_r^2} \left(\frac{\lambda}{4\pi d}\right)^4 |h_{\text{dl}}(t_k)|^2 |h_{\text{ul}}(t_k)|^2 \eta_{\text{mod}} \tag{3.26}$$

where $\eta_{\text{mod}} \in [0, 1]$ is the tag backscatter modulation efficiency which is defined in Section 3.2 and σ_r^2 is the power of the AWGN at the reader.

Another tag type is defined as ABEH RFID tag, which is the enhanced type of the conventional passive RFID tag as explained in Section 2.7. ABEH tag superimposes extra energy to the conventional passive tag's backscatter modulated signal with the help of its battery storage device such as capacitor. The square of the envelope of the received signal is given in equation (3.19) by evaluating ABEH tag structure and loss factors. In Appendix C, derivation of the received signal's instantaneous SNR at the reader in the ABEH structure is calculated. Thus,

$$\begin{aligned}\gamma_{\mathrm{RX,reader,ABEH}}(t_k) = &\frac{P_{\mathrm{TX,reader}} G_{\mathrm{reader}}^2 G_{\mathrm{tag}}^2}{\sigma_r^2} \left(\frac{\lambda}{4\pi d}\right)^4 |h_{\mathrm{dl}}(t_k)|^2 |h_{\mathrm{ul}}(t_k)|^2 \eta_{\mathrm{mod}} \\ &+ \frac{P_{\mathrm{amp},k} G_{\mathrm{reader}} G_{\mathrm{tag}}}{\sigma_r^2} \left(\frac{\lambda}{4\pi d}\right)^2 |h_{\mathrm{ul}}(t_k)|^2 \eta_{\mathrm{amp}}\end{aligned} \tag{3.27}$$

where η_{amp} is the efficiency of power amplifier (PA) and $P_{\mathrm{amp},k}$ is the amount of amplification power by feeding the PA of the ABEH tag at time slot k according to equation (3.19).

The final model of the instantaneous SNR at the reader is given in equation (3.27), which depends on the transmit power of the reader, the antenna gain of the reader and the tag, the distance between the tag and the reader, the operating frequency, and the channel fading coefficients regardless of the RFID tag type. The only difference between the conventional passive and the ABEH tag model is the power amplification that is utilized by the way of energy harvesting.

In equation (3.27), first term of the summation represents the instantaneous SNR at the reader that is caused by the conventional passive RFID tag response. In other words, the backscatter modulation produces the first term of the summation in the equation (3.27). The reason of the second term is the power amplification via energy harvesting. Thus, the second term symbolizes the instantaneous SNR caused by the PA of the ABEH tag which depends only on the UL channel. Therefore, equation (3.27) can be used both for the conventional passive and the ABEH type RFID systems. In order to employ equation (3.27) for the conventional passive case, assigning zero power amplification for all time slots is sufficient, i.e. $P_{\mathrm{amp},k} = 0, \forall k$.

4. DELAY-CONSTRAINED RFID MODEL

Multiple tags and possibly multiple readers generally forms a typical RFID system. The anti-collision interrogation model shows that the single tag selection can be achieved in one active time slot. Consequently evaluating the performance of a single tag is sufficient to analyze the overall RFID system thanks to the collision free model.

In an ordinary TDMA-based RFID system, the RFID reader continuously transmits CW signal, which also includes query command. Thus, each RFID tag experiences an active time slot in different time slots. In other saying, a tag in an active time slot means an idle time slot for the rest during that time slot According to that, only one tag is interrogated by the reader in each time slot. The frequency of the selection of a tag is named as "interrogation probability" in [1], which highly depends on the total number of tags in an RFID system. Increasing the total number of tags results in decreasing interrogation probability of a specific tag because the number of tags that can be queried is ascended. That is to say, growing the number of tags enhances the number of idle time slots per tag. With the help of these explanations, the conventional RFID system for a single tag can be depicted as stated below:

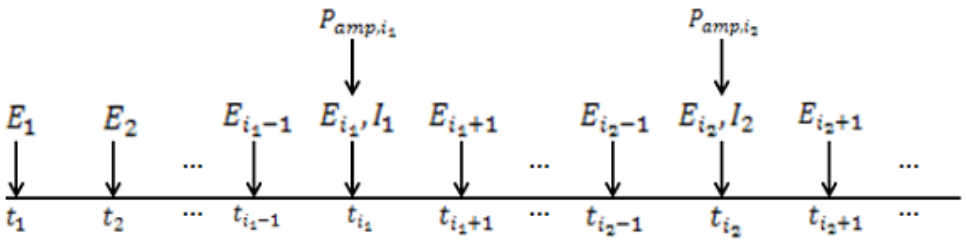

Figure 4.1. Delay-Constrained RFID Model

where E_k represents harvested energy at time slot k, $P_{\text{amp},k}$ is the utilized amplification power at time slot k and I_j symbolizes the jth interrogation of the tag. In this model, i_ℓ represents the interrogation time slot, where $\ell \in [1, 2, ..., N]$ and N is the total number of the interrogations. That is to say, the vector $\mathbf{i} = [i_1, i_2, ..., i_N]$ implies the time slots

of requests by the reader.

In a conventional RFID system, the tag must immediately give an answer to the read request coming from the reader. In other words, there is no time slot delay between the interrogation signal transmitted from the reader and the response of the tag. This is the reason of why system configuration in Figure 4.1 is called as "delay-constrained." In this type of RFID system model, the tag replies the query at once. Then if the SNR of the received backscatter modulated signal is high enough compared to the sensitivity or the SNR threshold of the reader device, it means that the tag is successfully read by the reader. Since the reader sends multiple requests at different time slots, the total number of successful detections of the tag turns out to be an important parameter. Instead of taking total number of detections as a performance measure, detection probability can be used. For this reason, time average of the read probability becomes a very crucial performance measure in the RFID systems. The read probability of a tag can be described as the ratio between the number of successful reads and the total number of interrogations by the reader. In the probabilistic domain, the read probability can be imagined as the probability of the received signal SNR at the reader is greater than the threshold SNR of the reader. Therefore, the average read probability can be denoted by

$$\overline{p}_{\text{read}} = \frac{1}{N} \sum_{k=1}^{N} Pr[\gamma_{\text{RX,reader,ABEH}}(t_{i_k}) \geq \gamma_{\text{th,reader}}] \tag{4.1}$$

where $\gamma_{\text{RX,reader,ABEH}}(t_{i_k})$ is the received signal's instantaneous SNR at the reader in time slot i_k, $\gamma_{\text{th,reader}}$ is the SNR threshold for the reader and $\overline{p}_{\text{read}}$ is the average read probability. Furthermore, $\gamma_{\text{RX,reader,ABEH}}(t_{i_k})$ is a random variable because the communication channel is random variable. Derivation of the average read probability under Rayleigh flat fading channel is implemented in Appendix D. Notice that under the frequency-flat Rayleigh fading channels with a priori knowledge of the downlink CSI for power allocation scenario [1], the received signal SNR can be seen as an exponen-

tially distributed random variable with the pdf given by

$$f_{\gamma_{\mathrm{RX,reader,ABEH}}}(\gamma(t_k)) = \frac{1}{\gamma_0(t_k)} e^{-\frac{\gamma(t_k)}{\gamma_0(t_k)}}, \qquad \gamma(t_k) > 0 \tag{4.2}$$

where

$$\gamma_0(t_k) = \gamma_{\mathrm{TX,reader}} \left(\frac{\lambda}{4\pi d}\right)^4 |h_{\mathrm{dl}}(t_k)|^2 \eta_{\mathrm{mod}} + \gamma_{\mathrm{amp},i_k} \left(\frac{\lambda}{4\pi d}\right)^2 \eta_{\mathrm{amp}} \quad .$$

4.1. Delay-Constrained Off-line Optimization

The concept of energy harvesting including the optimum transmission policies were investigated in [4–6, 97–101] etc. However, these works focused on finding the optimum transmission policies to maximize data rate or minimize the transmission time and so on. Maximizing the read probability with a similar fashion has not been investigated.

Within the optimization problem defined in this work, the average read probability is maximized under such limitations as energy causality, battery capacity and minimum required amplification power constraints. Accordingly, calculating the cost function of the optimization is the first step [102]. Since the objective function of the optimization problem is the average read probability, it should have a mathematical formula. Because of that the mathematical description of the average read probability is derived in Appendix F. Furthermore, it is assumed that all incoming energies are known beforehand, which means the downlink fading coefficients are known while performing optimization. Thus, *a priori* knowledge of the downlink channel state information makes the optimization problem "off-line". In [1], it is supposed that the tag should respond the read request immediately, which makes the RFID system delay-constrained. According to that, delay-constrained ABEH tag RFID system constraint

optimization problem is

$$\begin{aligned}
\underset{P_{\text{amp},i_k}}{\text{maximize}} \quad & \frac{1}{N}\sum_{k=1}^{N}\exp\Big(-\frac{a}{b_k+gP_{\text{amp},i_k}}\Big) \\
\text{s.t.} \quad & \sum_{k=1}^{i_\ell}E_k-\sum_{k=1}^{\ell}TP_{\text{amp},i_k}\le E_{\max}, \quad \ell=1,...,N \\
& \sum_{k=1}^{\ell}TP_{\text{amp},i_k}\le\sum_{k=1}^{i_\ell}E_k, \qquad \ell=1,...,N \\
& P_{\text{amp},i_\ell}\ge 0 \qquad \ell=1,...,N
\end{aligned} \tag{4.3}$$

where $a=P_{\text{th,reader}}$, $b_k=P_{\text{TX,reader}}|h_{\text{dl}}(t_{i_k})|^2\big(\frac{\lambda}{4\pi d}\big)^4\eta_{\text{mod}}$, $g=\big(\frac{\lambda}{4\pi d}\big)^2\eta_{\text{amp}}$ and N is the number of active time slots.

The first constraint implies the battery capacity, where the energy at the storage device at any time must be less than or equal to the maximum energy capacity. The energy causality constraint is addressed in the second constraint, which shows that the consumed energy must be less than or equal to the harvested energy at any time slot. The last constraint is the minimum amplification power constraint because any power must be nonnegative.

4.1.1. Concavity Condition of the Delay-Constrained Objective Function

The objective function, $f_0(x_1,...,x_N)$, is defined as

$$\begin{aligned}
f_0(x_1,...,x_N)=f_0(\mathbf{x}) &= \frac{1}{N}\sum_{k=1}^{N}exp\big(-\frac{a}{b_k+gP_{\text{amp},i_k}}\big) \\
&= \frac{1}{N}\left[e^{-\frac{a}{b_1+gx_1}}+e^{-\frac{a}{b_2+gx_2}}+...+e^{-\frac{a}{b_N+gx_N}}\right]
\end{aligned} \tag{4.4}$$

where $x_k=P_{\text{amp},i_k}$ and $\mathbf{x}=[x_1,...,x_N]^T$. In order to check its concavity, the Hessian of the objective function must be negative semidefinite matrix [102], i.e. $\nabla^2_{\mathbf{x}}f_0(\mathbf{x})\preceq 0$. Consequently, the first derivative and the Hessian of the objective function are

calculated as

$$\begin{aligned}
\nabla_{\mathbf{x}} f_0(\mathbf{x}) &= \left[\frac{\partial f_0(\mathbf{x})}{\partial x_1}, \frac{\partial f_0(\mathbf{x})}{\partial x_2}, ..., \frac{\partial f_0(\mathbf{x})}{\partial x_N}\right] \\
&= \frac{1}{N}\left[\frac{ag}{(b_1+gx_1)^2} e^{-\frac{a}{b_1+gx_1}}, ..., \frac{ag}{(b_N+gx_N)^2} e^{-\frac{a}{b_N+gx_N}}\right] \\
\nabla^2_{\mathbf{x}} \mathrm{f}_0(\mathbf{x}) &= \begin{bmatrix} \frac{\partial^2 f_0(\mathbf{x})}{\partial x_1^2} & \frac{\partial^2 f_0(\mathbf{x})}{\partial x_1 \partial x_2} & \cdots & \frac{\partial^2 f_0(\mathbf{x})}{\partial x_1 \partial x_N} \\ \vdots & \vdots & \ddots & \vdots \\ \frac{\partial^2 f_0(\mathbf{x})}{\partial x_N \partial x_1} & \frac{\partial^2 f_0(\mathbf{x})}{\partial x_N \partial x_2} & \cdots & \frac{\partial^2 f_0(\mathbf{x})}{\partial x_N^2} \end{bmatrix}
\end{aligned} \tag{4.5}$$

where

$$\begin{aligned}
\frac{\partial^2 f_0(\mathbf{x})}{\partial x_k^2} &= -\frac{2ag^2(b_k+gx_k)}{(b_k+gx_k)^4} e^{-\frac{a}{b_k+gx_k}} + \frac{a^2g^2}{(b_k+gx_k)^4} e^{-\frac{a}{b_k+gx_k}} \\
&= ag^2 \frac{e^{-\frac{a}{b_k+gx_k}}[a-2(b_k+gx_k)]}{(b_k+gx_k)^4} \\
\frac{\partial^2 f_0(\mathbf{x})}{\partial x_k \partial x_j} &= 0, k \neq j \quad .
\end{aligned} \tag{4.6}$$

Therefore, the Hessian of the cost function could be reduced to

$$\nabla^2_{\mathbf{x}} f_0(\mathbf{x}) = \frac{ag^2}{N} diag\Big(\frac{e^{-\frac{a}{b_k+gx_k}}[a-2(b_k+gx_k)]}{(b_k+gx_k)^4}\Big) \preceq 0, k = 1, ..., N \quad .$$

Since $\frac{ag^2}{M} \geq 0$, $e^{-\frac{a}{b_k+gx_k}} \geq 0$ and $(b_k+gx_k)^4 \geq 0, \forall k = 1, ..., N$, the subsequent equation must hold in order to supply concavity of the objective function.

$$\begin{aligned}
[a-2(b_k+gx_k)] &\leq 0 \qquad ,\forall k = 1, ..., N \\
\frac{\frac{a}{2}-b_k}{g} &\leq x_k \qquad ,\forall k = 1, ..., N \\
\frac{a-2b_k}{2g} &\leq x_k \qquad ,\forall k = 1, ..., N \\
\frac{P_{\text{th,reader}} - 2P_{\text{TX,reader}}(\frac{\lambda}{4\pi d})^4 |h_{\text{dl}}(t_{i_k})|^2 \eta_{\text{mod}}}{2(\frac{\lambda}{4\pi d})^2 \eta_{\text{amp}}} &\leq P_{\text{amp},i_k}, \forall k = 1, ..., N
\end{aligned} \tag{4.7}$$

which is the implicit constraint of the optimization problem. Changing the implicit constraint to the explicit one converts the optimization problem to

$$\begin{aligned}
\underset{x_k}{\text{maximize}} \quad & \frac{1}{N}\sum_{k=1}^{N}\exp\Big(-\frac{a}{b_k+gx_k}\Big) \\
\text{s.t.} \quad & \sum_{k=1}^{i_\ell}E_k-\sum_{k=1}^{\ell}Tx_k\le E_{\max} \quad ,\ell=1,...,N \\
& \sum_{k=1}^{\ell}Tx_k\le\sum_{k=1}^{i_\ell}E_k \quad ,\ell=1,...,N \\
& x_\ell\ge\max\Big(0,\frac{a-2b_\ell}{2g}\Big) \quad ,\ell=1,...,N \ .
\end{aligned} \tag{4.8}$$

Last constraint guarantees the concavity of the objective function. Since maximizing the sum of exponentials with fractional exponents is a complicated problem, first order Taylor expansion is applied to the exponential function, where the objective function and its first order Taylor expansion is shown in Figure 4.2.

Applying first order Taylor expansion [103] to the exponential function, we have

$$\exp\left(-\frac{a}{b_k+gx_k}\right)\approx 1-\frac{a}{b_k+gx_k},\ k=1,\dots,N \ .$$

As a result, the optimization problem turns out to be

$$\begin{aligned}
\underset{x_k}{\text{minimize}} \quad & \frac{1}{N}\sum_{k=1}^{N}\frac{a}{b_k+gx_k} \\
\text{s.t.} \quad & \sum_{k=1}^{i_\ell}E_k-\sum_{k=1}^{\ell}Tx_k\le E_{\max} \quad ,\ell=1,...,N \\
& \sum_{k=1}^{\ell}Tx_k\le\sum_{k=1}^{i_\ell}E_k \quad ,\ell=1,...,N \\
& x_\ell\ge\max\Big(0,\frac{a-2b_\ell}{2g}\Big) \quad ,\ell=1,...,\mathrm{N} \ .
\end{aligned} \tag{4.9}$$

The main optimization problem is now changed to the sum of linear fractional optimization, and the objective function is still concave with the same constraints.

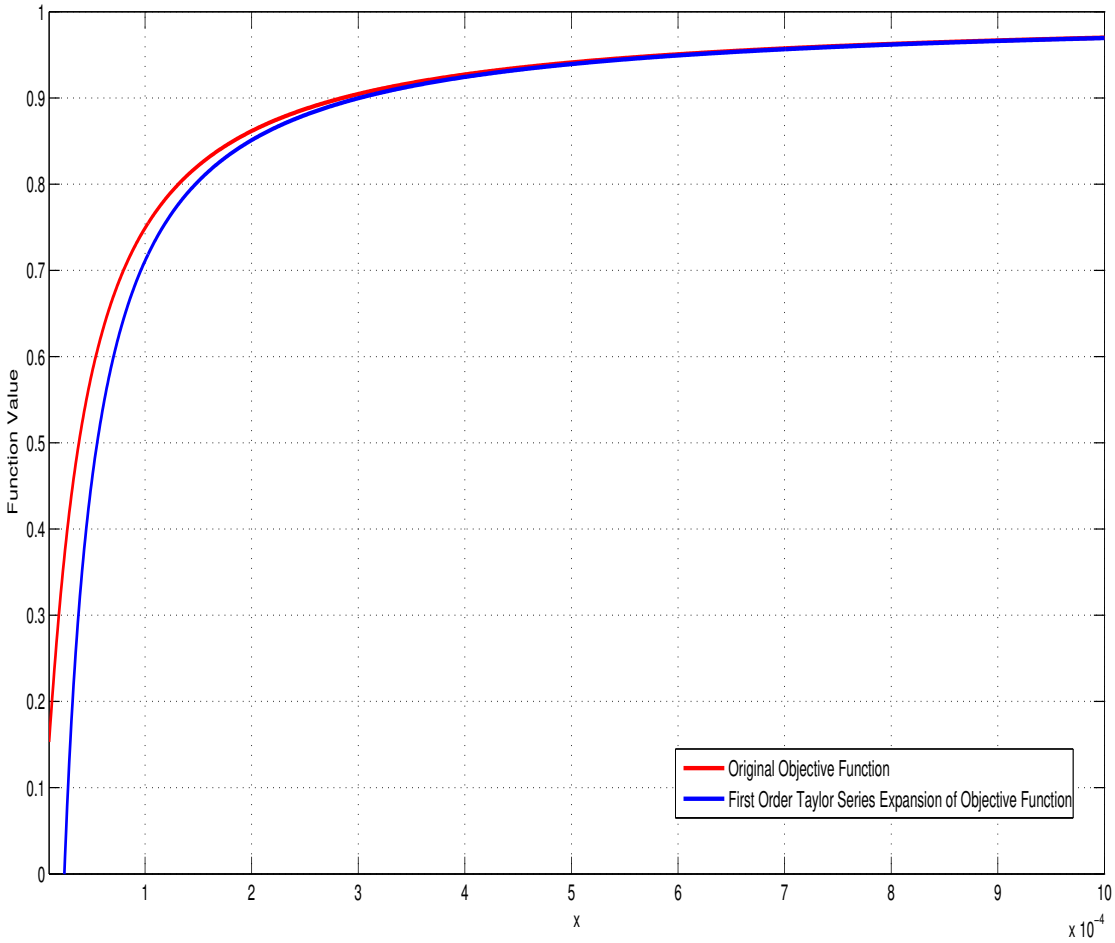

Figure 4.2. Objective function and its Taylor expansion approximation

An alternative to equation (4.9) is seeking the amplification power, x_k, that maximizes the smallest denominator among all $b_k + gx_k, k = 1, \ldots, N$. That is,

$$\underset{x_k}{\text{minimize}} \frac{1}{N} \sum_{k=1}^{N} \frac{a}{b_k + gx_k} \sim \underset{x_k}{\text{maximize}} \left\{ \min_k \left[b_k + gx_k \right] \right\} \quad .$$

The concave maximization problem in (4.9) is reduced to a max-min problem, which can be solved more easily than the sum of linear fractional programming. The

new optimization problem can be transformed to the following one:

$$\begin{aligned} \underset{x_k}{\text{maximize}} \quad & \min_k \left\{ b_k + g x_k \right\} \\ \text{s.t.} \quad & \sum_{k=1}^{i_\ell} E_k - \sum_{k=1}^{\ell} T x_k \leq E_{\max} \quad , \ell = 1, ..., N \\ & \sum_{k=1}^{\ell} T x_k \leq \sum_{k=1}^{i_\ell} E_k \quad , \ell = 1, ..., N \\ & x_\ell \geq \max\Big(0, \frac{a - 2b_\ell}{2g}\Big) \quad , \ell = 1, ..., N \end{aligned} \tag{4.10}$$

which is still concave with the same convex set of constraints. Therefore, the solution of the maximization problem is unique.

4.1.2. Slackness Conditions of the Delay-Constrained Off-line Optimization

The Lagrangian of the delay-constrained off-line optimization can be set up as

$$\begin{aligned} \mathcal{L} = & \min_k \left\{ b_k + g x_k \right\} \\ & + \sum_{j=1}^{N} \lambda_{1j} \Bigg(\sum_{k=1}^{i_j} E_k - \sum_{k=1}^{j} T x_k - E_{\max} \Bigg) \\ & + \sum_{j=1}^{N} \lambda_{2j} \Bigg(\sum_{k=1}^{j} T x_k - \sum_{k=1}^{i_j} E_k \Bigg) \\ & + \sum_{j=1}^{N} \lambda_{3j} \left[x_j - \max\left(0, \frac{a - 2b_j}{2g}\right) \right] \quad . \end{aligned} \tag{4.11}$$

The complementary slackness conditions are

$$\lambda_{1j} \Bigg(\sum_{k=1}^{i_j} E_k - \sum_{k=1}^{j} T x_k - E_{\max} \Bigg) = 0, \forall j \tag{4.12}$$

$$\lambda_{2j} \Bigg(\sum_{k=1}^{j} T x_k - \sum_{k=1}^{i_j} E_k \Bigg) = 0, \forall j \tag{4.13}$$

$$\lambda_{3j}\left[x_j - max\Big(0, \frac{a-2b_j}{2g}\Big)\right] = 0, \forall j \quad . \tag{4.14}$$

The delay-constrained optimization problem can be solved using numerical methods because a closed from solution to (4.11)-(4.14) is not possible. In order to solve the optimization problem numerically, CVX program [104] is used. The slackness conditions are explained next in order to evaluate the scenarios performed by the ABEH RFID tag.

Case 1 ($\lambda_{2j} \neq 0$): Due to the slackness condition (4.13), we necessarily have

$$\sum_{k=1}^{i_j} E_k = \sum_{k=1}^{j} T x_k \quad .$$

This case is possible when the harvested energy exactly equals to the consumed one from the battery, and there is no energy flow to subsequent slots. Thus, this case might be named as "no energy flow to next slots."

Case 2 ($\lambda_{2j} = 0$): In this situation, $\sum_{k=1}^{i_j} E_k$ must be different than $\sum_{k=1}^{j} T x_k$. In other words, the harvested energy exceeds the used one because of the energy causality. Since $\sum_{k=1}^{i_j} E_k > \sum_{k=1}^{j} T x_k$, there is energy flow to the next time slot. Therefore, this case might be called as "maximum or expanding capacity" for the battery. This case can be further evaluated based on two scenarios:

Case 2.1 ($\lambda_{1j} \neq 0$): From (4.12),

$$\sum_{k=1}^{i_j} E_k - \sum_{k=1}^{j} T x_k - E_{\max} = 0 \quad ,$$

which means that the difference between the harvested and used energies is equal to the battery capacity. In other saying, energy storage limit is reached. If $x_k = 0$, then all the incoming energy from the reader between $(k-1)^{th}$ and k^{th} interrogations is stored, and the maximum battery capacity is reached. That is to say, due to the poor

channel conditions, all the energy transmitted by the reader is intentionally stored. If $x_k \neq 0$, then some part of the incoming energy coming from the reader is stored and the rest is used for power amplification. At the end, the energy in the battery is reached its maximum value. This scenario is named as "maximum capacity" because the battery capacity is reached whether power amplification is performed or not.

Case 2.2 ($\lambda_{1j} = 0$): In this scenario,

$$\sum_{k=1}^{i_j} E_k - \sum_{k=1}^{j} T x_k - E_{\max} \neq 0 \quad .$$

Because of the capacity constraint, $\sum_{k=1}^{i_j} E_k - \sum_{k=1}^{j} T x_k < E_{\max}$, i.e., the difference between the harvested and used energy is less than the battery capacity. In other words, energy is transferred to the subsequent slot but storage capacity is not exceeded.

If $x_k = 0$, then all the incoming energy from the reader between $(k-1)^{th}$ and k^{th} interrogations is stored and power amplification is not realized. This situation implies a "disabled" state of amplification due to the poor uplink channel conditions during the active time slot.

If $x_k > \max\left(0, \frac{a-2b_k}{2g}\right)$, then some of the harvested energy is used for amplification but the remaining amount is diverted to the battery. Since the power amplification is performed, this case might be called as "enabled" state of the power amplification. This case occurs when uplink fading level in active time slot is favorable enough to store some of the incoming energy during idle time slots.

Regardless of the power amplification situation, the energy in the battery increases. Consequently, Case 2.2 is called as "expanding capacity" state.

4.2. Amplification Decision Algorithm for Delay-Constrained Model

The PA of the ABEH tag is used to boost the power of backscatter modulated signal in order to enhance the read probability. However, the ABEH tag must make a decision of whether extra power is added on the backscatter signal or not. In addition, if the ABEH tag decides power amplification, the amount of that power must be determined by the tag. Thus the logic unit of the ABEH tag takes a decision of whether amplification is performed or not, and it also calculates the required amount of power that is superimposed on the backscatter modulated signal. In order to calculate the amount of required amplification power, current DL and UL channel conditions must be known or estimated beforehand in the active time slot. Proposed amplification decision algorithm assumes that the both channel fading coefficients are previously known by the ABEH tag, which makes the algorithm off-line. In addition to the channel fading coefficients, the reader's transmit power, antenna gains, AWGN power at the reader, distance between the tag and the reader, efficiency of PA, efficiency of backscatter modulation and operating frequency are also assumed to be known priorly by the ABEH tag. All these values are constant during each transmission. For this reason, the only random parameters are the UL and DL fading channel coefficients. Note that the only UL channel fading coefficient is known in the active time slots.

In the idle time slots, energy is obviously harvested according to the equation (3.23). The proposed amplification decision algorithm only operates in the active time slots differently from the algorithm in [1]. In other words, the harvested energy during the idle time slots and the energy harvesting parameters such as η_{DC} are not take into account by the ABEH tag, which is the one of the main advantages over [1]. The logic unit becomes a part of an activity when the time slot is active. At these slots, the logic unit calculates the necessary amplification power to be read with the help of known incoming signal energy, UL fading coefficient, distance, carrier frequency, inefficiency values and the reader sensitivity according to the equation (3.27).

The calculation of required amplification power can be given by

$$\gamma_{\text{th,reader}} \geq \frac{P_{\text{TX,reader}} G_{\text{reader}}^2 G_{\text{tag}}^2}{\sigma_r^2} \left(\frac{\lambda}{4\pi d}\right)^4 |h_{\text{dl}}(t_k)|^2 |h_{\text{ul}}(t_k)|^2 \eta_{\text{mod}} + \frac{P_{\text{amp},k} G_{\text{reader}} G_{\text{tag}}}{\sigma_r^2} \left(\frac{\lambda}{4\pi d}\right)^2 |h_{\text{ul}}(t_k)|^2 \eta_{\text{amp}} \tag{4.15}$$

where minimum required amplification power, i.e. $P_{\text{amp},k}$, will be estimated with this equation. The calculation of the necessary amplification power is performed via equation (4.15) by equating right hand side of the equation to the reader sensitivity. The result of this equity yields minimum value of the amplification power.The ABEH tag calculates the required amplification power and checks the state of the battery. If the available energy at the storage device is sufficient, then the logic unit decides in the favor of power amplification. In other words, the logic unit conveys the permission of power amplification and the amount of amplification energy information to the energy storage device and the PA. Otherwise, the tag stores the received signal energy even the time slot is active. Therefore, the proposed amplification power policy completely depends on the battery evolution and the channel conditions. Furthermore, the logic unit of the ABEH tag behaves like an on/off switch, which is easy to implement in hardware. The tag enters on-state mode when the channel and the battery conditions can be opportunistically used, and the tag chooses off-state mode when the necessary conditions are not met. That is to say, the tag lifts the power of the transmitted signal if the channel is well enough. Since exceeding the reader SNR threshold yields successful read, considering equation (4.15) is sufficient whether the power amplification will be used or not. Note that the RFID system is assumed as delay-constrained which means that the tag must respond immediately when it receives the query command from the reader. The following table visualizes the proposed off-line algorithm in the delay-constrained RFID system :

Require Prior Knowledge of $h_{\mathrm{ul}}(t_k)$, G_{reader}, G_{tag}, $\gamma_{\mathrm{th,reader}}$, $P_{\mathrm{TX,reader}}$, d, f, η_{amp} and η_{mod}.
if Time Slot==Idle **then**
  Store Incoming Energy
end if
if Time Slot==Active **then**
  Calculate Required Amplification Energy
  if Insufficient Energy in the Battery **then**
    Store Incoming Energy
  end if
  if Sufficient Energy in the Battery **then**
    Use Calculated Energy from the Battery
  end if
end if

Figure 4.3. Amplification Decision Algorithm for Delay-Constrained RFID System.

In [1], MDP was performed by the logic unit, which is a much more complex decision method for the logic unit. The UL and DL fading channel coefficients are also known beforehand by the tag in both active and idle time slots in [1], which is not the case in the proposed algorithm. In this thesis, only the UL fading coefficient should be priorly known in the active slots. DL fading coefficient is extracted from the incoming signal energy in the active time slot. In addition, interrogation probability is also assumed to be known in [1] whereas proposed algorithm is much more simpler than MDP method, and the proposed algorithm doesn't require the prior knowledge of interrogation probability, DL and UL channel coefficients in idle time slots. Therefore the proposed power amplification decision algorithm requires less information compared to [1].

5. DELAY-TOLERANT RFID MODEL

In Chapter 4, the delay-constrained RFID system model is explained where the ABEH tag must reply the request immediately. On the other hand, if the ABEH tag has an opportunity to hang on its reply for a while, then it may increase its read chance by selecting more favorable time slot. In this model, ABEH tag doesn't have to respond to an incoming interrogation of the reader immediately. To put it differently, the tag can delay the response signal, which is why this system is called as "delay-tolerant." When the reader interrogates the tag, ABEH tag may choose the time slot, which has suitable channel conditions in order to be read. The delay-tolerant RFID model is illustrated in Figure 5.1 as stated below:

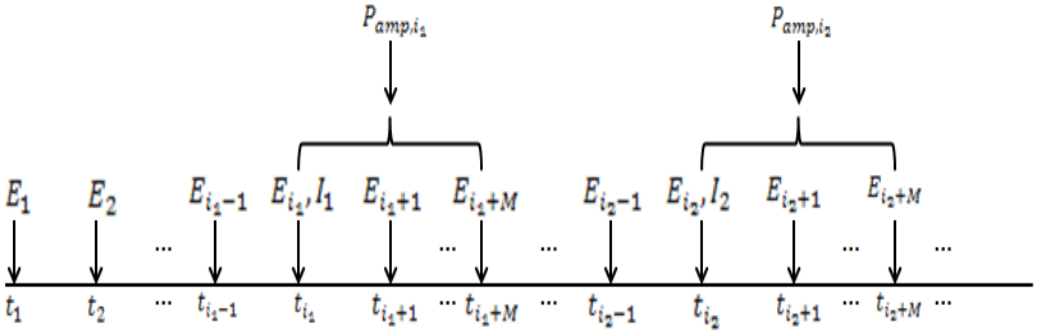

Figure 5.1. Delay-Tolerant RFID Model

where E_k represents harvested energy at time slot k, $P_{\text{amp},k}$ is the utilized amplification power at time slot k and I_j symbolizes the jth interrogation of the tag where N is the total number of the interrogations. In this model, i_ℓ represents the interrogation time slot where $\ell = [1, 2, ..., N]$. In other words, the vector $\mathbf{i} = [i_1, i_2, ..., i_N]$ implies the time slots of the requests of the reader. Moreover, M represents the number of allowed delay slots. Consequently, the tag can wait M time slots so as to respond. In other saying, M is the maximum number of time slots that the tag can wait. Suppose that the reader sends z^{th} request to the tag, which means that the time slot is t_{i_z}. Thus, the time slot that the tag replies must be between t_{i_z} and $t_{i_{z+M}}$.

The maximum value of M is the number of time slots between two consecutive interrogations, and $M = 0$ implies that the model is delay-constrained as in Chapter 4. Once the tag decides in the favor of power amplification within the allowed delay time interval, the same procedure is performed as in Section 4.1. The only difference is about time slot of reply signal. If the backscattered signal SNR exceeds the threshold SNR value of the reader, then the tag is read successfully. Furthermore, the tag opportunistically harvests the energy of the incoming signals by the reader until the time slot of amplification of backscatter signal. That is to say, the tag stores energy except when it transmits back the respond signal. In delay-tolerant scenario, collision-free model is not considered which is left as a future work.

Presuming that the tag transmits within M time slots to seek the channel that has the optimum received SNR in the frequency-flat Rayleigh fading scenario with prior knowledge of the downlink CSI for power allocation scenario [1]. Then the probability distribution of the received SNR in the delay-tolerant model, i.e. $\gamma_{\mathrm{RX,reader}}(t_k)$, becomes

$$f_{\gamma_{\mathrm{RX,reader,ABEH}}}(\gamma(t_k)) = \sum_{u=0}^{M} \frac{1}{\gamma_u(t_k)} e^{-\frac{\gamma(t_k)}{\gamma_u(t_k)}} \prod_{v \neq u}^{M} (1 - e^{-\frac{\gamma(t_k)}{\gamma_v(t_k)}}), \quad \gamma > 0 \qquad (5.1)$$

where

$$\gamma_u(t_k) = \gamma_{\mathrm{TX,reader}} \left(\frac{\lambda}{4\pi d}\right)^4 |h_{\mathrm{dl}}(t_{k+u})|^2 \eta_{\mathrm{mod}} + \gamma_{\mathrm{amp},i_{k+u}} \left(\frac{\lambda}{4\pi d}\right)^2 \eta_{\mathrm{amp}}, \quad u = 0, 1, \ldots, M \ .$$

5.1. Delay-Tolerant Off-line Optimization

In the delay-tolerant scheme, the tag can choose any time slot between the interrogation time slot and the maximum allowed time slot. Since the tag can select an optimum time slot within the allowed time window, the average read probability improves. The tag reduces its amplification power by choosing the time slot that will preserve maximum energy in the battery for future use. However, selecting the optimum time slot is a diversity problem [84]. The receiver diversity is generally employed

with antenna array configuration, where the system includes multiple antennas.On the other hand, our system has only one antenna at the tag. Nevertheless, time array is selected as the source of diversity instead of antenna array setup. Therefore, choosing the optimum time slot is also diversity problem. Only the source of diversity changes.

There are many ways to implement the receiver diversity, and one of them is selection combining (SC). In this method, the combiner chooses the antenna that has maximum received SNR. The selection diversity is based on choosing the channel, which has the highest received signal power in MIMO configuration at the receiver side [84]. Since the time array is utilized instead of antenna array in the delay-tolerant RFID model, the combiner selects the time slot that has maximum received SNR in our case. The approach based on the selective diversity may be applied to the delay-tolerant RFID model with the prior knowledge of M uplink time slots after the interrogation instant. For this reason, the average read probability of the SC-based time diversity approach is

$$\overline{p}_{\text{read}} = \frac{1}{N}\sum_{k=1}^{N} \Pr\left[\max\left(\gamma_{\text{RX,reader}}(t_{i_k}), ..., \gamma_{\text{RX,reader}}(t_{i_k+M})\right) \geq \gamma_{\text{th,reader}}\right]. \tag{5.2}$$

The derivation of the average read probability of the SC-based time diversity approach is explained in Appendix G. Accordingly, the optimization of the average read probability in the delay-tolerant model is given as

$$
\begin{aligned}
\underset{x_{k,u}}{\text{maximize}} \quad & 1-\frac{1}{N}\sum_{k=1}^{N}\left[\prod_{u=0}^{M}\left[1-\exp\Big(-\frac{a}{b_{k,u}+gx_{k,u}}\Big)\right]\right], \\
\text{s.t.} \quad & \sum_{k=1}^{i_\ell+u} E_k - \sum_{k=1}^{\ell} Tx_{k,u} \le E_{\max}, && u=0,...,M, \ell=1,...,N \\
& \sum_{k=1}^{\ell} Tx_{k,u} \le \sum_{k=1}^{i_\ell+u} E_k, && u=0,...,M, \ell=1,...,N \\
& x_{\ell,u} \ge \max\Big(0, \frac{a-2b_{\ell,u}}{2g}\Big) && u=0,...,M, \ell=1,...,N
\end{aligned}
\tag{5.3}
$$

where $a=\gamma_{\text{th,reader}}, b_{k,u}=\gamma_{\text{TX,reader}}|h_{dl}(t_{i_k+u})|^2\big(\frac{\lambda}{4\pi d}\big)^4\eta_{\text{mod}}, g=\big(\frac{\lambda}{4\pi d}\big)^2\eta_{\text{amp}}$ and $x_{k,u}=\gamma_{\text{amp,i}_\text{k}+\text{u}}$. Equivalently,

$$
\begin{aligned}
\underset{x_{k,u}}{\text{minimize}} \quad & \frac{1}{N}\sum_{k=1}^{N}\left[\prod_{u=0}^{M}\left[1-\exp\Big(-\frac{a}{b_{k,u}+gx_{k,u}}\Big)\right]\right], \\
\text{s.t.} \quad & \sum_{k=1}^{i_\ell+u} E_k - \sum_{k=1}^{\ell} Tx_{k,u} \le E_{\max}, && u=0,...,M, \ell=1,...,N \\
& \sum_{k=1}^{\ell} Tx_{k,u} \le \sum_{k=1}^{i_\ell+u} E_k, && u=0,...,M, \ell=1,...,N \\
& x_{\ell,u} \ge \max\Big(0, \frac{a-2b_{\ell,u}}{2g}\Big) && u=0,...,M, \ell=1,...,N.
\end{aligned}
\tag{5.4}
$$

Since the objective function of the (5.4) is complicated in order to perform optimization, the optimization problem is rearranged to reduce the complexity of the maximization. By applying first-order Taylor series expansion, the delay-tolerant optimization problem becomes

$$
\begin{aligned}
\underset{x_{k,u}}{\text{minimize}} \quad & \frac{1}{N}\sum_{k=1}^{N}\left[\prod_{u=0}^{M}\left[1-\left(1-\frac{a}{b_{k,u}+gx_{k,u}}\right)\right]\right], \\
\text{s.t.} \quad & \sum_{k=1}^{i_\ell+u} E_k - \sum_{k=1}^{\ell} Tx_{k,u} \le E_{\max}, && u=0,...,M, \ell=1,...,N \\
& \sum_{k=1}^{\ell} Tx_{k,u} \le \sum_{k=1}^{i_\ell+u} E_k, && u=0,...,M, \ell=1,...,N \\
& x_{\ell,u} \ge \max\left(0, \frac{a-2b_{\ell,u}}{2g}\right) && u=0,...,M, \ell=1,...,N.
\end{aligned} \tag{5.5}
$$

Thus, the delay-tolerant optimization problem simplified as

$$
\begin{aligned}
\underset{x_{k,u}}{\text{minimize}} \quad & \frac{1}{N}\sum_{k=1}^{N}\prod_{u=0}^{M}\frac{a}{b_{k,u}+gx_{k,u}}, \\
\text{s.t.} \quad & \sum_{k=1}^{i_\ell+u} E_k - \sum_{k=1}^{\ell} Tx_{k,u} \le E_{\max}, && u=0,...,M, \ell=1,...,N \\
& \sum_{k=1}^{\ell} Tx_{k,u} \le \sum_{k=1}^{i_\ell+u} E_k, && u=0,...,M, \ell=1,...,N \\
& x_{\ell,u} \ge \max\left(0, \frac{a-2b_{\ell,u}}{2g}\right) && u=0,...,M, \ell=1,...,N.
\end{aligned} \tag{5.6}
$$

The same simplification procedure can be applied to the delay-tolerant optimization problem as in delay-constrained case. An alternative to equation (5.6) is seeking the amplification power, $x_{k,u}$, that maximizes the smallest denominator among all $b_{k,u}+gx_{k,u}, k=1,\ldots,N$,where $u=0,\ldots,M$. That is,

$$
\underset{x_{k,u}}{\text{minimize}} \frac{1}{N}\sum_{k=1}^{N}\prod_{u=0}^{M}\frac{a}{b_{k,u}+gx_{k,u}} \sim \underset{x_{k,u}}{\text{maximize}} \left\{\min_{k}\left\{\prod_{u=0}^{M}\left[b_{k,u}+gx_{k,u}\right]\right\}\right\} \ .
$$

Consequently, the optimization problem in (5.6) is reduced to a max-min problem. Since the energy causality, battery capacity and minimum required amplification power constraints are the same as in delay-constrained model, the same simplifying steps are

applied as in the delay-constrained optimization model in Section 4.1.1 and Section 4.1.2. The SC-based optimization problem of the delay-tolerant model is given by

$$\begin{aligned} \underset{x_{k,u}}{\text{maximize}} \quad & \left\{ \min_{k} \left[\prod_{u=0}^{M} b_{k,u} + g x_{k,u} \right] \right\}, \\ \text{s.t.} \quad & \sum_{k=1}^{i_\ell+u} E_k - \sum_{k=1}^{\ell} T x_{k,u} \leq E_{\max}, \quad u = 0, ..., M, \ell = 1, ..., N \\ & \sum_{k=1}^{\ell} T x_{k,u} \leq \sum_{k=1}^{i_\ell+u} E_k, \qquad u = 0, ..., M, \ell = 1, ..., N \\ & x_{\ell,u} \geq \left(0, \frac{a - 2b_{\ell,u}}{2g}\right) \qquad u = 0, ..., M, \ell = 1, ..., N. \end{aligned} \tag{5.7}$$

Note that the complementary slackness conditions and the scenarios by the tag are also the same as in delay-constrained model because the constraints are the same.

5.2. Amplification Decision Algorithm for Delay-Tolerant Model

The delay-tolerant RFID system model is a completely new phenomena since it has not been studied before in the literature in terms of RFID system. Behavior of the tag in the idle time slots in delay-tolerant system is the same with the delay-constrained case. The tag harvests the incoming signal energies during the idle time slots. In active time slots, tag calculates required amplification power as in delay-constrained case with the help of priorly known UL fading coefficients. The proposed amplification decision algorithm for delay-tolerant ABEH RFID model is visualized in Figure 5.2.

The calculation of required amplification power is also the same with the delay-constrained case, where equation (4.15) is the basis of the process. After the calculation of the required amplification power, the tag checks whether the battery has sufficient energy or not. If sufficient energy is available within the storage device, then the tag performs power amplification with a calculated amount. However, there may be energy shortage in the battery in order to be read by the reader. Since the tag doesn't have to reply the reader immediately in delay-tolerant case, the tag may want to transmit

its response packet later. In each allowed time slot, it calculates required amplification power and checks its battery state in order to decide whether power amplification will be performed or not. In other words, the tag performs amplification decision procedure in each allowed time slot until sufficient conditions are met. If the channel conditions are well enough to be read by the reader, the response packet is transmitted by the tag even if it has a chance to wait.

Additionally, the proposed algorithm forces the tag to stop waiting when the communication channel is favorable. The time slot that the amplification is performed must be between the interrogation time slot and the maximum allowed time slot. If any of time slots between those two are not favorable to be read, the ABEH tag harvests energy of the incoming signals in these time slots. In other words, if the tag doesn't have enough energy for amplification for whole M time slots, it stores the energy of the incoming signals in the proposed amplification decision algorithm for delay-tolerant RFID model. Because prior knowledge of UL fading coefficient is necessary to calculate the power, it is assumed that the tag knows it previously, which makes RFID model off-line. Unlike the delay-constrained case, the tag can choose an optimum UL and DL channel conditions to be successfully read in an off-line policy. The read probability of the tag enhances by giving delay tolerance to it because the tag can select optimum time slot within allowed delay tolerance. Actually, the tag reduces its amplification power by choosing ultimate time slot, which will increase its stored energy in the battery for the future use.

Require Prior Knowledge of $h_{\mathrm{ul}}(t_{i_k})-h_{\mathrm{ul}}(t_{i_k+M})$, G_{reader}, G_{tag}, $\gamma_{\mathrm{th,reader}}$, $P_{\mathrm{TX,reader}}$, d, f, η_{amp} and η_{mod}.

if Time Slot==Idle **then**

  Store Incoming Energy

end if

if Time Slot==Active **then**

  i=0;

  while $i \leq M$ **do**

    i=i+1;

    Calculate Required Amplification Energy

    if Insufficient Energy in the Battery **then**

      Store Incoming Energy

    end if

    if Sufficient Energy in the Battery **then**

      Use Calculated Energy from the Battery

      break

    end if

  end while

end if

Figure 5.2. Amplification Decision Algorithm for Delay-Tolerant RFID System.

6. SIMULATION RESULTS

In this chapter, numerical results are provided to show the read range improvement of ABEH tag with respect to conventional passive tags in both delay-constrained case. In addition, dramatic advance of read probability in delay-tolerant RFID model is also provided compared to delay-constrained one. Corresponding upper bounds and the optimization results of both cases are also provided. DL and UL channels are supposed to be statistically independent Rayleigh channels. Another assumption is upon the distance. The path length of UL channel is assumed the same with the distance of DL channel.

In each simulation, harvested energy is quantized according to predetermined number of quantization levels. Quantization of the energy in the battery is implemented according to the battery capacity as in [1]. Furthermore, the quantization step size is determined as $0.22 \cdot 10^{-8}$ J, which means different $E_{\max}$ values have different number of quantization levels. Some of the parameters are assumed to be the same for each simulation. These parameters and its values are $\eta_{\text{amp}} = 0.2$, $\eta_{\text{mod}} = 0.2$, $\eta_{\text{DC}} = 0.4$, $P_{\text{TX,reader}} = 4$ W, $\gamma_{\text{th,reader}} = -67$ dBm, $G_{\text{reader}} = 1$, $G_{\text{tag}} = 1$, $f_0 = 915$ MHz and $T = 10$ ms which are constant for all frames. During the simulations, the interrogation probability has a binomial distribution except the simulations that contains optimization. While performing optimization simulations, the uniform distribution is implemented for the interrogation probability.

Four different $E_{\max}$ values are selected in which these are 0.14 μJ, 0.56 μJ, 1.12 μJ and 2.24 μJ. In addition to these ABEH tags, conventional passive RFID tag is also included in simulations where it doesn't have any energy storage devices, i.e. $E_{\max} = 0$ J.

The upper bounds in Figure 6.1 are calculated by assigning used amplification power to the battery size value, i.e. $P_{\text{amp},k} = E_{\max}/T$, for each active time slot in the read probability equation, which is derived in Appendix D. Consequently, any

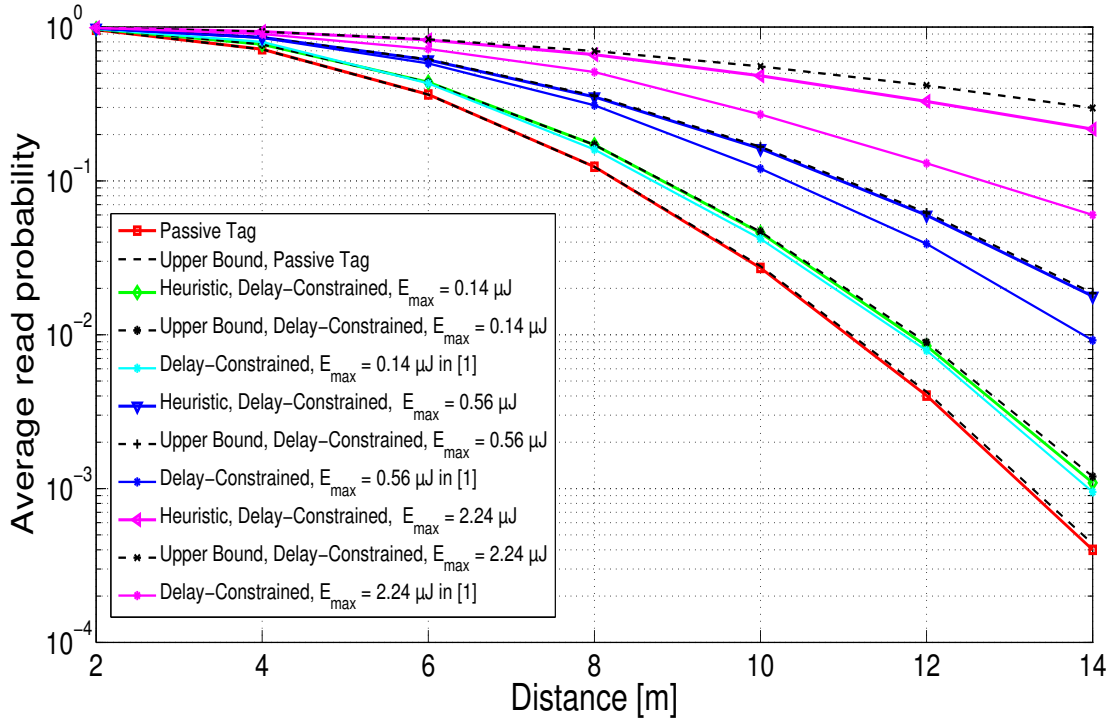

Figure 6.1. Average read probability of passive and ABEH tags versus distance between tag and reader for different energy storage sizes in delay-constrained case, together with the results in [1].

backscatter modulated signal power policy must lie under this curve because it is assumed that the tag always adds its maximum energy to the conventional passive tag power.

Note that zero amplification power, i.e. $P_{\text{amp},k} = 0$ for each active time slot converts ABEH tag to the conventional passive RFID tag. Therefore, the upper bound for conventional passive tag is also illustrated in Figure 6.1. Another research subject in Figure 6.1 is the effect of $E_{\max}$ on read probability. The amount of energy capacity has an impact on the read range. As can be seen from the figure, increasing the battery capacity results in better read range and/or read probability performance even if the value of the battery size is small. Since growing storage device capacity can harvest a higher amount of energy, more power generates better read chance for the tag. In addition, interrogation probability for Figure 6.1 is selected as 0.1.

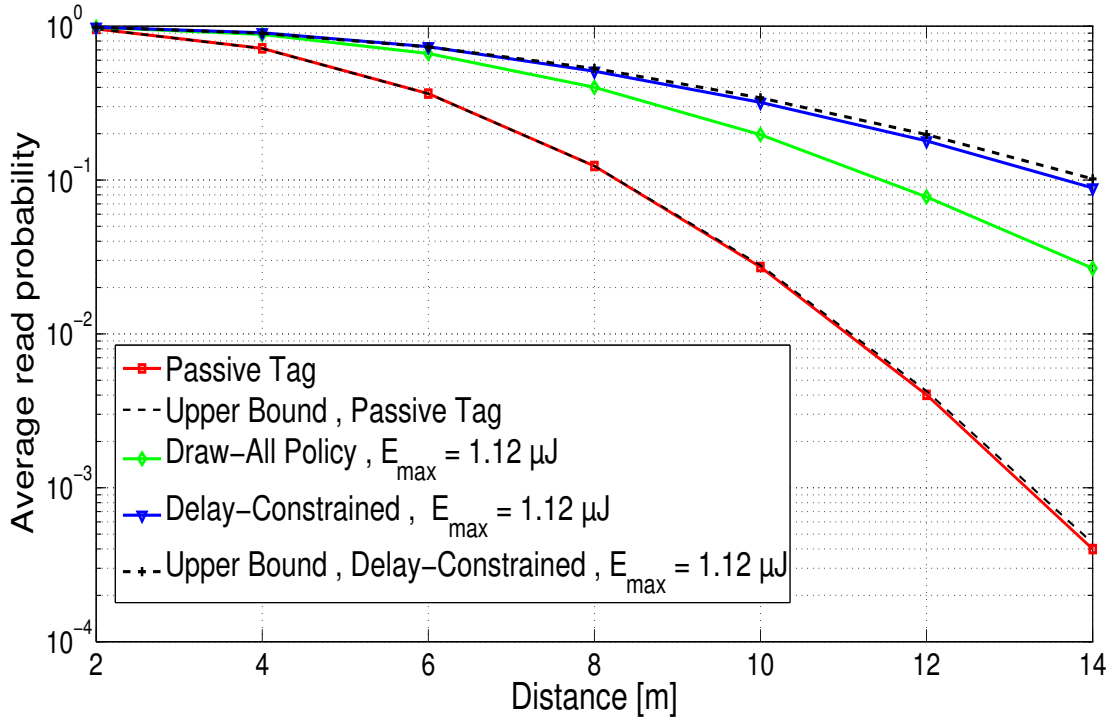

Figure 6.2. Average read probability of ABEH tag versus distance between tag and reader for $E_{\max}$=1.12 μJ with the results of draw-all policy in delay-constrained case.

The performance of the proposed algorithm at different battery capacity levels is nearly the same with the corresponding upper bounds themselves. The reason of the gap between the upper bound and the heuristic result is caused by the assumption of a fully charged battery in each active time slot in calculation of upper bound. Since the battery is empty initially and the harvested energy may not convey the battery state to its maximum value until the next active time slot in real environment, the gap between them is reasonable. However, one important observation about the gap is that the decreasing battery size results in a smaller the gap which is also understandable because the chance of reaching the maximum storage level for a higher battery is much harder than the lower battery capacity.

The draw-all policy is such that all harvested energy is employed as an amplification power in each active time slot. On the other hand, Figure 6.2 shows that this is a suboptimal solution. Therefore, the advantage of utilizing a logic unit with

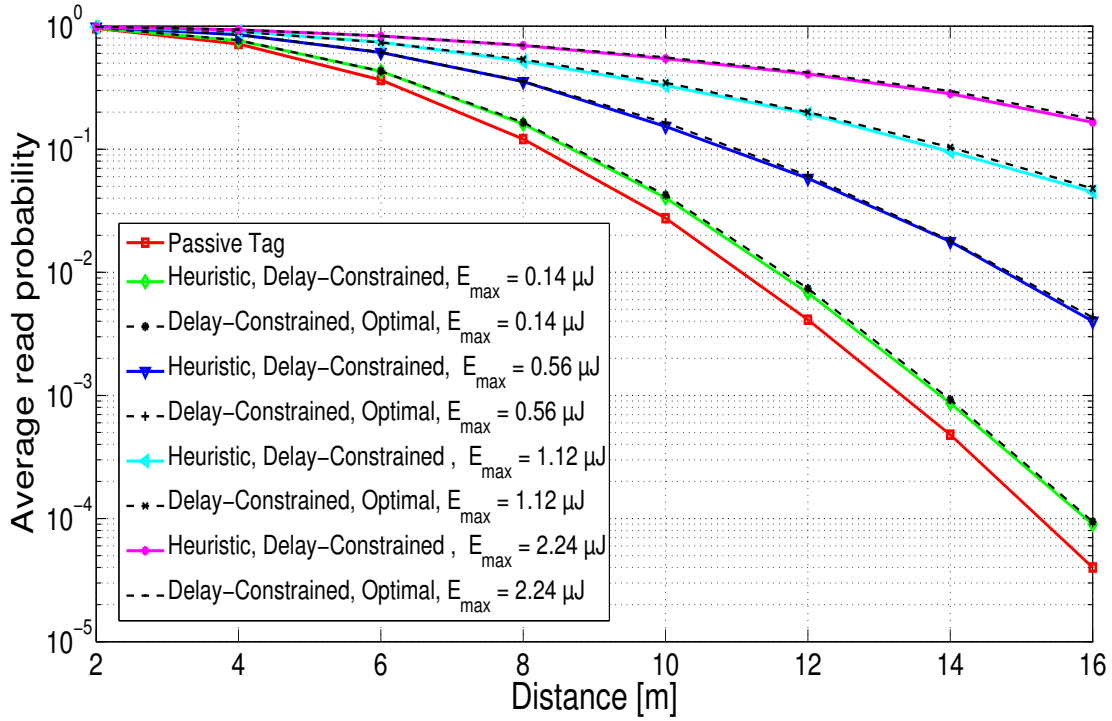

Figure 6.3. Average read probability of ABEH tag versus distance between tag and reader for different $E_{\max}$ values in delay-constrained case with their corresponding optimal values.

a smart algorithm gives better results. Since the gap between the draw-all policy and maximum achievable read probability is high, different policies can be applied in order to enhance the performance.

In Figure 6.3, the ABEH tag is considered with optimal read probability values, which are obtained by numerically solving the optimization problem in (4.10). While performing optimization problem, the CVX program [104] is used to find the numerical results. The proposed algorithm's results are very close to the corresponding optimal curves. Note that the interrogation rate is selected as $p_{\text{int}} = 0.02$ while solving the optimization problem.

In Figure 6.4, delay-tolerant case is implemented for various number of delay slots. Increasing the delay slot number enhances the read probability because the chance of facing with a good channel increases. The maximum number of delay slot refers to

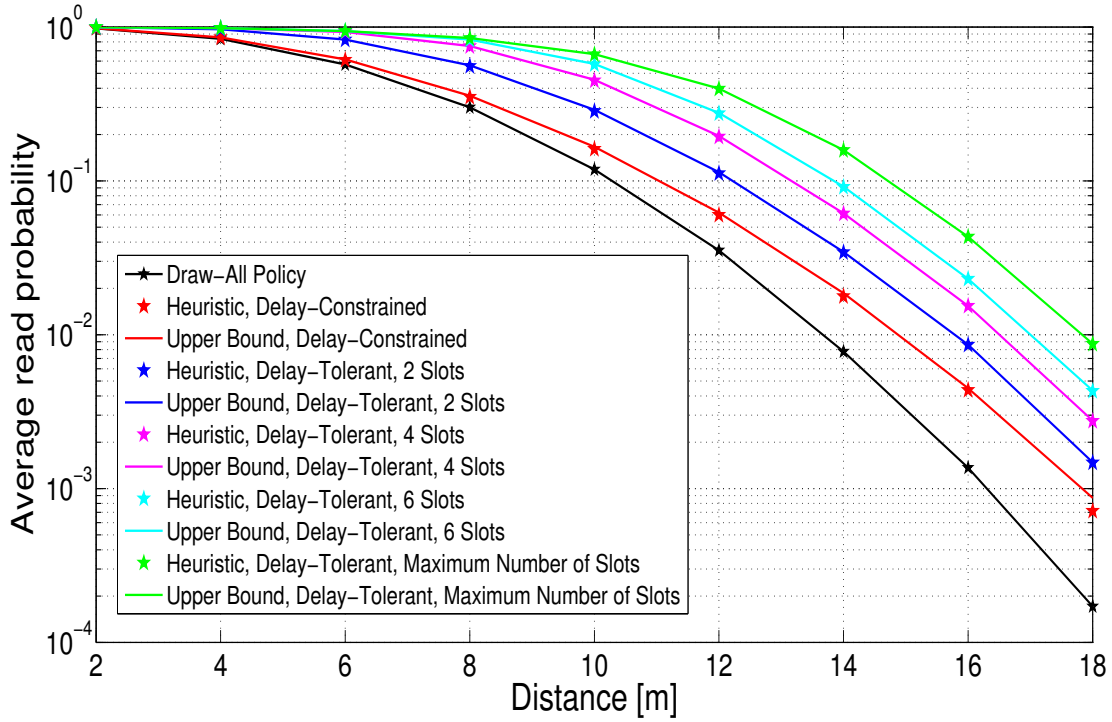

Figure 6.4. Average read probability of ABEH tag versus distance between tag and reader for $E_{\max}$=0.56 μJ and $p_{\text{int}} = 0.1$ in draw-all policy and delay-constrained and delay-tolerant cases with their corresponding upper bounds.

the difference between two subsequent active time slots. In other words, ABEH tag can wait until the next active time slot in order to perform backscatter amplification regardless of the number of slots between two consecutive active time slots. Since the maximum achievable number of delay is the number of difference between two consecutive active time slots, the maximum achievable read probability for an ABEH tag is the upper bound for maximum number of delay slots in delay tolerant case which is the uppermost line in Figure 6.4.

In addition to delay-tolerant ABEH RFID model, the draw-all policy is also implemented to show the effects of different policies upon the read range. The draw-all policy means that the tag imposes its total harvested energy on the backscatter signal in a delay-constrained fashion. That is to say, when the time slot is active, the tag adds its all harvested energy up to now onto the backscatter signal. Since the draw-all

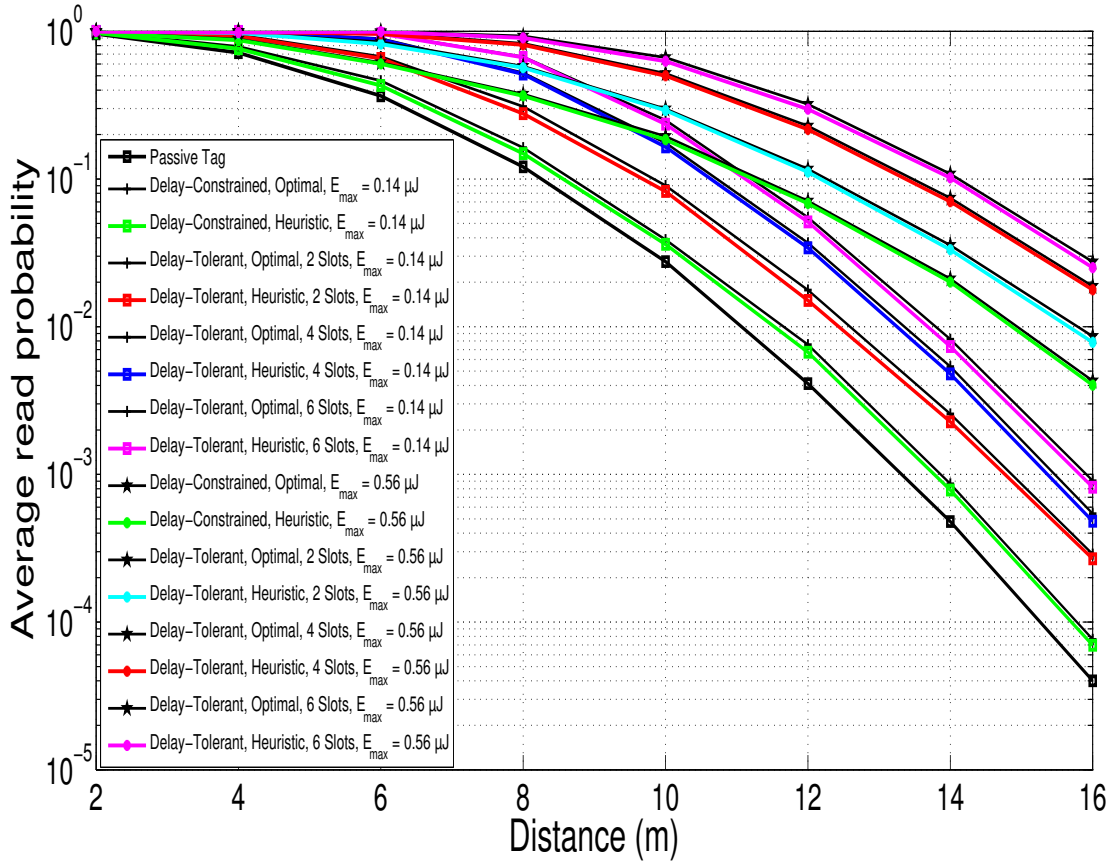

Figure 6.5. Average read probability of ABEH tag versus distance between tag and reader for $p_{\text{int}} = 0.025$ in delay-constrained and delay-tolerant cases with their corresponding optimization results.

policy doesn't use harvested energies reasonably, this policy's read range and/or read probability is lower than the proposed algorithms even if compared system is delay-constrained. The read range difference between the draw-all policy and proposed delay-constrained algorithm shows that the harvested energies should be used carefully and logically in order to increase the read range. Note that, in simulations, upper bounds for Rayleigh flat fading channel is also calculated by setting $P_{\text{amp},k} = E_{\max}/T$. From the Figure 6.4, the upper bound curve and the proposed algorithm results are nearly the same for $E_{\max} = 0.56$ μJ. Since the upper bound is the maximum achievable curve for the ABEH RFID tag, proposed off-line algorithm for both delay-tolerant and delay-constrained cases are the efficient algorithms for ABEH RFID tag.

The optimization problem of the average read probability with constraints are defined in equation (5.7) for delay-tolerant model. By evaluating this optimization problem with CVX program [104] and performing proposed algorithm, Figure 6.5 is obtained. As the figure implies, the proposed algorithm results are close to their corresponding optimal value. Since the proposed algorithm is an off-line policy, the gap between the optimal values and heuristic (proposed) algorithm results is very small.

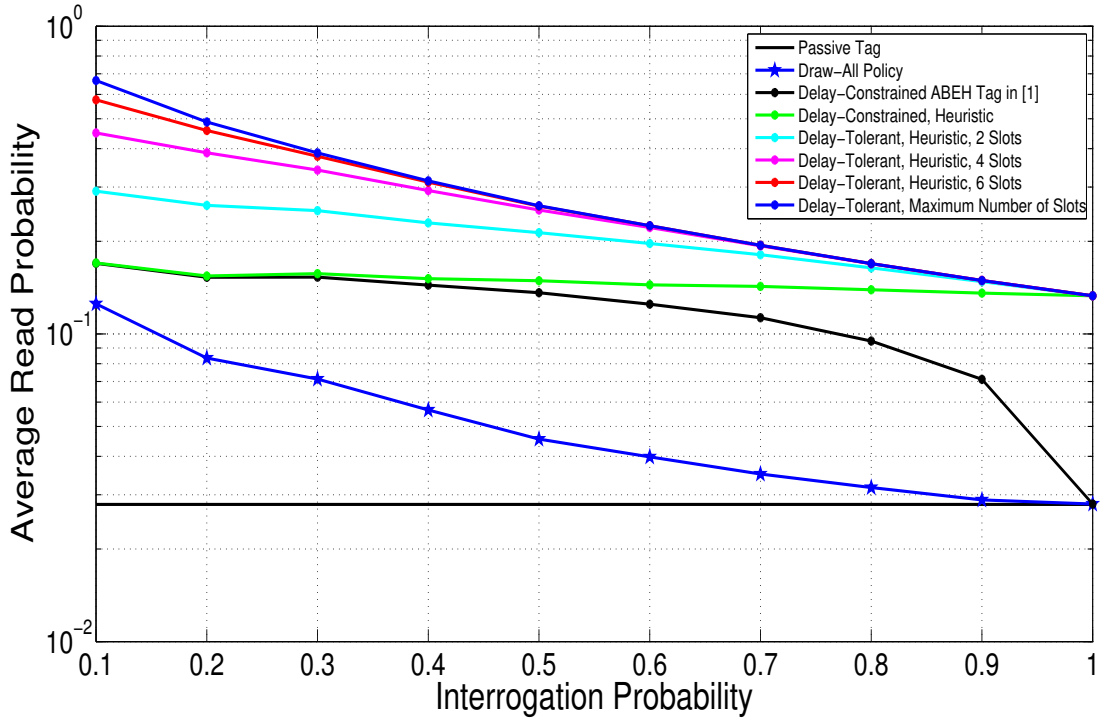

Figure 6.6. Average read probability of ABEH tag versus interrogation probability for $E_{\max} = 0.56$ μJ and $d = 10$ m in delay-constrained and delay-tolerant case

The effects of interrogation probability on the read probability is evaluated in Figure 6.6. Both the delay-constrained and delay-tolerant models are included. In addition, the draw-all policy and conventional passive tag policy is also investigated in order to make a comparison. As the interrogation probability converges to one, the number of idle time slots converges to zero.

The draw-all policy converges to the conventional passive tag's read probability as the interrogation probability goes to one because the number of the idle time slots

are decreasing, which diminishes the harvested energies. When the interrogation probability is one, all the time slots are active time slots. Thus, there is no idle time slot in order to harvest energy which causes that the tag behaves like a conventional passive tag. In other words, since opportunistically energy harvesting is not performed due to the lack of an idle time slot, the tag can be considered as a tag without energy storage device, which makes it the conventional passive tag. Note that all curves must be above the conventional passive tag because it doesn't have an energy storage device.

In order to show the difference when the interrogation probability converges to one, two different delay-constrained algorithms are implemented. One delay-constrained algorithm is the proposed algorithm, which is defined in Section 4.2 where the ABEH tag harvests the incoming signal energy if battery of the tag doesn't have sufficient energy to perform the successful transmission. The other delay-constrained algorithm supposes that the incoming request signal from the reader must be transmitted back even if the channel conditions are not favorable. In other words, if there is a shortage of energy at the battery of the tag for a successful communication, the tag behaves like a conventional passive tag when it is interrogated, which implies the tag transmits back incoming signal without performing power amplification. Therefore, the only difference between two delay-constrained algorithms causes from their behavior in active time slots when the energy storage device does not have enough energy for power amplification so as to achieve a successful communication. While the proposed algorithm stores the incoming request signal energy at inappropriate conditions, the other one reflects back incoming request signal without performing power amplification as a conventional passive tag.

Accordingly, the effect of interrogation probability on two delay-tolerant algorithms can be seen from the figure. Since proposed algorithm opportunistically harvests energy under poor channel conditions, it utilizes these energies in good channel conditions when the power amplification is required. On the other hand, the other algorithm which is the proposed algorithm in [1] converges to the conventional passive RFID tag when the interrogation probability converges to one. Although the delay-constrained algorithm in [1] assumes prior knowledge of channel coefficients, this algorithm does

not benefit from any prior knowledge of channel condition. For this reason, the read probability of proposed algorithm reduces very slowly in the case of increasing interrogation probability but the performance of the algorithm in [1] reduces faster than the proposed algorithm. Furthermore, while the proposed algorithm approaches to a read probability value which is higher than the conventional passive one, the algorithm in [1] converges to the read probability of conventional passive tag as the interrogation probability converges to one.

Another result comes from the difference between the delay-constrained and delay-tolerant models. Low interrogation probability has more time slots between two consecutive active time slots than the high interrogation probability because the frequency of request of a specific tag reduces under low interrogation probability. Therefore, the delay-tolerant ABEH RFID model performs much better than the delay-constrained model under low interrogation probability. This is reasonable because the more the difference between two subsequent active time slots increases the chance of power amplification. As the interrogation probability ascends, delay-tolerant model converges to the delay-constrained one. That is to say, decreasing gap between two subsequent active time slots due to increasing interrogation probability restricts allowed tag's response time limit. When the interrogation probability is one, there is no idle time slot. That means the difference between two consecutive active time slots is zero. Therefore, interrogation probability with one implies the delay-constrained case, which is proven by the Figure 6.6.

The energy evolution during 100 time slots is shown in Figure 6.7 with the 0.8 interrogation probability. The upper bound is obviously $E_{\max}$ value because the capacity of the battery is limited with that value. Since energy in the battery can not be negative value, lower bound is zero, which is the depleted battery or battery-free case. The whole harvested energies during idle time slots are utilized in an active time slot in order to amplify the backscatter signal in the draw-all policy. For this reason, in each active time slot the battery must be depleted as in Figure 6.7, which is obviously suboptimal policy. The energy evolution difference between the proposed algorithm and the algorithm in [1] can be seen from the figure. Energy in the battery in the

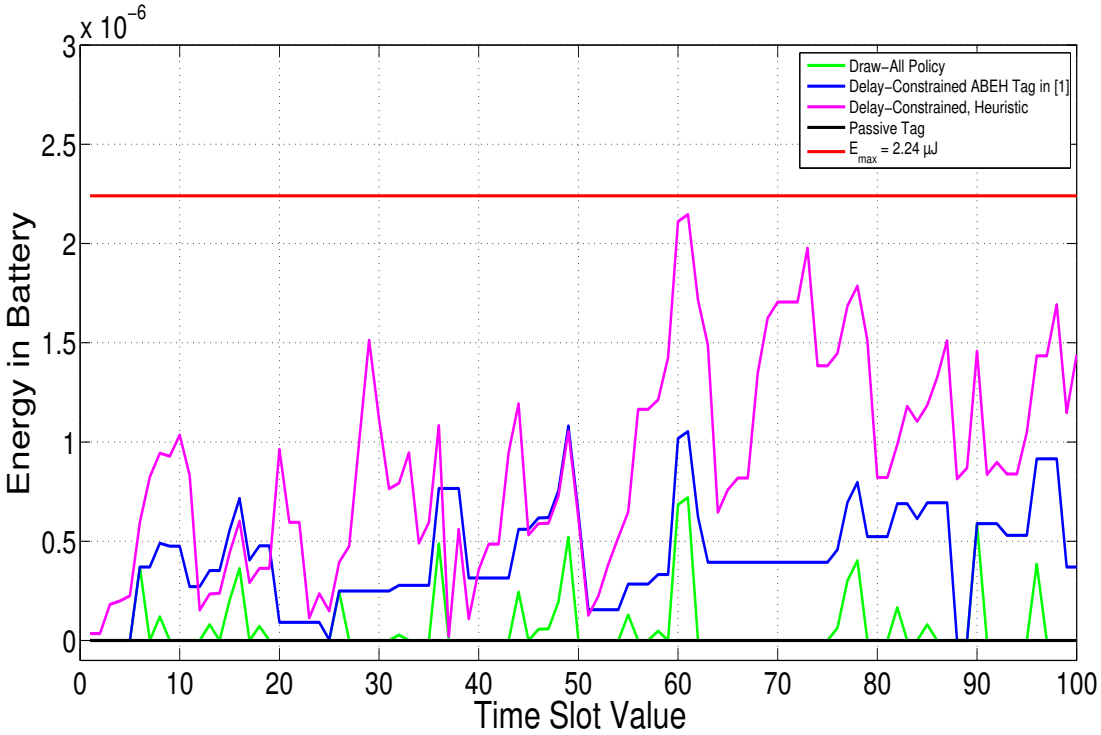

Figure 6.7. Energy evolution of a tag with $E_{\max}$=2.24 μJ and $d = 8$ m

proposed algorithm is generally higher than the other one, which creates more chance of successful transmission. For example, when considering the time slots between 65 and 75, there are series of active time slots because of high interrogation probability. The proposed algorithm opportunistically stores the energies if the battery condition is not good enough to respond to the reader. On the other hand, other algorithm reflects back the incoming signal even though the tag knows that transmitted signal can not be successful. Because of that procedure, energy state in the other algorithm is constant but the proposed algorithm may utilize these harvested energies in later time slots.

7. CONCLUSION

In this thesis, an ABEH-based RFID architecture is proposed in which the RFID tags are equipped with energy harvesting and storing units. Delay-constrained and delay-tolerant transmission scenarios are considered for the RFID tags, and theoretical upper bounds for the average read probability are derived under the slow-fading Rayleigh channel model for both scenarios. Moreover, two heuristic algorithms that make amplification decisions based on the average read probability calculations are presented. Simulations under different battery capacity constraints are conducted, where the results indicate significant advantages obtained by the use of the proposed architectures together with practical power allocation algorithms. The amount of *a priori* knowledge of channel fading coefficient is extremely reduced compared to [1]. Decision algorithm in [1] requires prior knowledge for both DL and UL channels for all time slots. However, in this thesis only the UL CSI is required at the active time slots for backscatter modulated signal power level determination. Therefore, the proposed algorithm leads to lower memory requirements related to [1]. Proposed power amplification decision algorithm has also significantly low complexity compared to the MDP based algorithm in [1]. Theoretical average read probability is derived under slow-fading Rayleigh channel, and the simulation results show that the results of the proposed algorithm is in tight agreement with the theoretical optimal values. For this reason, the proposed algorithm may be used as an off-line optimal curve which reduces computational complexity markedly. Giving the chance of delay to the tag extremely increases average read probability and superiority of the delay-tolerant model. Therefore delay-tolerant model reduces the energy requirement remarkably.

For a future work, channel model can be changed or anti-collision model for the delay-tolerant model can be investigated. Furthermore, different time slot selection approaches can be researched in the delay-tolerant structure.

REFERENCES

1. Iannello, F., O. Simeone and U. Spagnolini, "Energy Management Policies for Passive RFID Sensors with RF-Energy Harvesting", *IEEE International Conference on Communications (ICC)*, pp. 1–6, 2010.

2. Lu, X., P. Wang, D. Niyato, D. I. Kim and Z. Han, "Wireless Networks With RF Energy Harvesting: A Contemporary Survey", *IEEE Communications Surveys and Tutorials*, Vol. 17, pp. 757–789, 2015.

3. Zungeru, A. M., L. M. Ang, S. Prabaharan and K. P. Seng, "Radio frequency energy harvesting and management for wireless sensor networks", *Green Mobile Devices Netw.: Energy Opt. Scav. Tech.,CRC Press*, pp. 341–368, 2012.

4. Ozel, O., K. Tutuncuoglu, J. Yang, S. Ulukus and A. Yener, "Resource management for fading wireless channels with energy harvesting nodes", *Proceedings IEEE INFOCOM*, pp. 456–460, 2011.

5. Tutuncuoglu, K., A. Yener and S. Ulukus, "Optimum Policies for an Energy Harvesting Transmitter Under Energy Storage Losses", *IEEE Journal on Selected Areas in Communications*, Vol. 33, pp. 467–481, 2015.

6. Yang, J. and S. Ulukus, "Optimal Packet Scheduling in an Energy Harvesting Communication System", *IEEE Transactions on Communications*, Vol. 60, pp. 220–230, 2011.

7. Ulukus, S., A. Yener, E. Erkip, O. Simeone, M. Zorzi, P. Grover and K. Huang, "Energy Harvesting Wireless Communications: A Review of Recent Advances", *IEEE Journal on Selected Areas in Communications*, Vol. 33, pp. 360–381, 2015.

8. Stockman, H., "Communication by means of reflected power", *Proceedings of the IRE*, Vol. 36, pp. 1196–1204, 1948.

9. Vannucci, G., A. Bletsas and D. Leigh, "A software-defined radio system for backscatter sensor networks", *IEEE Transactions on Wireless Communications*, Vol. 7, pp. 2170–2179, 2008.

10. Kimionis, J., A. Bletsas and J. N. Sahalos, "Bistatic backscatter radio for power-limited sensor networks", *IEEE Global Communications Conference (GLOBECOM)*, Vol. 7, pp. 353–358, 2013.

11. Huynh, N. V., D. T. Hoang, X. Lu, D. Niyato, P. Wang and D. I. Kim, "Ambient backscatter communications: A contemporary survey", *arXiv:1712.04804 [cs.NI]*, December 2017.

12. Kim, S. H. and D. I. Kim, "Hybrid backscatter communication for wireless-powered heterogeneous networks", *IEEE Transactions on Wireless Communications*, Vol. 16, pp. 6557–6570, 2017.

13. Lu, X., P. Wang, D. Niyato, D. I. Kim and Z. Han, "Wireless networks with RF energy harvesting: A contemporary survey", *IEEE Communications Surveys and Tutorials*, Vol. 17, pp. 757–789, 2015.

14. Lu, X., P. Wang, D. Niyato, D. I. Kim and Z. Han, "Wireless charging technologies: Fundamentals, standards, and network applications", *IEEE Communications Surveys and Tutorials*, Vol. 18, pp. 1413–1452, 2016.

15. Ju, H. and R. Zhang, "Throughput maximization in wireless powered communication networks", *IEEE Transactions on Wireless Communications*, Vol. 13, pp. 418–428, 2014.

16. Lyu, B., H. Guo, Z. Yang and G. Gui, "Throughput maximization for hybrid backscatter assisted cognitive wireless powered radio networks", *IEEE Internet of Things Journal*, Vol. 5, pp. 2015–2024, 2018.

17. Lu, X., D. Niyato, H. Jiang, D. I. Kim, Y. Xiao and Z. Han, "Ambient backscat-

ter assisted wireless powered communications", *IEEE Wireless Communications*, Vol. 25, pp. 170–177, 2018.

18. Bansal, R., "Coming soon to a Wal-Mart near you", *IEEE Microwave and Guided Wave Letters*, Vol. 45, pp. 105–106, 2003.

19. Landt, J., "The history of RFID", *IEEE Potentials*, Vol. 24, pp. 8–11, 2005.

20. Ozel, O., K. Tutuncuoglu, J. Yang, S. Ulukus and A. Yener, "Transmission with Energy Harvesting Nodes in Fading Wireless Channels: Optimal Policies", *IEEE Journal on Selected Areas in Communications*, Vol. 29, pp. 1732–1743, 2011.

21. Xu, J. and R. Zhang, "Throughput Optimal Policies for Energy Harvesting Wireless Transmitters with Non-Ideal Circuit Power", *IEEE Journal on Selected Areas in Communications*, Vol. 32, pp. 322–332, 2014.

22. Devillers, B. and D. Gündüz, "A general framework for the optimization of energy harvesting communication systems with battery imperfections", *IEEE Journal on Communications and Networks*, Vol. 14, pp. 130–139, 2012.

23. Tutuncuoglu, K. and A. Yener, "Optimum Transmission Policies for Battery Limited Energy Harvesting Nodes", *IEEE Transactions on Wireless Communications*, Vol. 11, pp. 1180–1189, 2012.

24. Want, R., "An introduction to RFID technology", *IEEE Pervasive Computing*, Vol. 5, pp. 25–33, 2006.

25. Nikitin, P. V., K. Rao and S. Lazar, "An Overview of Near Field UHF RFID", *IEEE International Conference on RFID*, pp. 167–174, 2007.

26. Finkenzeller, K., *RFID Handbook: Radio-Frequency Identification Fundamentals and Applications*, John Wiley & Sons, Inc., 2000.

27. Chen, S. and V. Thomas, "Optimization of inductive RFID technology", *Proceed-*

ings of the 2001 IEEE International Symposium on Electronics and the Environment, pp. 82–87, 2001.

28. Rao, K. V. S., "An overview of backscattered radio frequency identification system (RFID)", *IEEE Asia Pacific Microwave Conference*, Vol. 3, pp. 746–749, 1999.

29. Chawla, V. and D. S. Ha, "An overview of passive RFID", *IEEE Communications Magazine*, Vol. 45, pp. 11–17, 2007.

30. Carrez, F., R. Stolle and J. Vindevoghel, "A low-cost active antenna for short-range communication applications", *IEEE Antennas and Propagation Magazine*, Vol. 8, pp. 215–217, 1998.

31. Nikitin, P. and K. Rao, "Antennas and Propagation in UHF RFID Systems", *IEEE International Conference on RFID*, pp. 277–288, 2008.

32. Nikitin, P. and K. Rao, "Performance limitations of passive UHF RFID systems", *IEEE Antennas and Propagation Society International Symposium*, pp. 1011–1014, 2006.

33. Padhi, S., N. Karmakar, C. Law and S. Aditya, "A dual polarized aperture coupled circular patch antenna using a C-shaped coupling slot", *IEEE Transactions on Antennas and Propagation*, Vol. 51, pp. 3295–3298, 2003.

34. Marrocco, G., "Gain-optimized self-resonant meander line antennas for RFID applications", *IEEE Antennas and Wireless Propagation Letters*, Vol. 2, pp. 302–305, 2003.

35. Rao, K., P. Nikitin and S. Lam, "Antenna design for UHF RFID tags: a review and a practical application", *IEEE Transactions on Antennas and Propagation*, Vol. 53, pp. 3870–3876, 2005.

36. Chiu, S., I. Kipnis, M. Loyer, J. R. . D. Westberg, J. Johansson and P. Johansson,

"A 900 MHz UHF RFID Reader Transceiver IC", *IEEE Journal of Solid-State Circuits*, Vol. 42, pp. 2822–2833, 2007.

37. Zhang, J., Z. Xie, S. Lai and Z. Wu, "A design of RF receiving circuit of RFID reader", *Proceedings of International Conference on Microwave and Millimeter Wave Technology*, pp. 406–409, 2004.

38. Karthaus, U. and M. Fischer, "Fully integrated passive UHF RFID transponder IC with 16.7 micrometer minimum RF input power,", *IEEE Journal of Solid-State Circuits*, Vol. 38, pp. 1602–1608, 2003.

39. Marrocco, G., "The art of UHF RFID antenna design: impedance-matching and size-reduction techniques", *IEEE Antennas and Propagation Magazine*, Vol. 50, pp. 66–79, 2008.

40. Vita, G. D. and G. Iannaccone, "Design criteria for the RF section of UHF and microwave passive RFID transponders", *IEEE Transactions on Microwave Theory and Techniques*, Vol. 53, pp. 2978–2990, 2005.

41. Nikitin, P. and K. Rao, "Theory and measurement of backscattering from RFID tags", *IEEE Antennas and Propagation Magazine*, Vol. 48, pp. 212–218, 2006.

42. Engels, D. and S. Sarma, "The reader collision problem", *IEEE International Conference on Systems, Man and Cybernetics*, Vol. 3, p. 6, 2002.

43. Hale, W., "Frequency assignment: Theory and applications", *Proceedings of the IEEE*, Vol. 68, pp. 1497–1514, 1980.

44. Katzela, I. and M. Naghshineh, "Channel assignment schemes for cellular mobile telecommunication systems: A comprehensive survey", *IEEE Communications Surveys and Tutorials*, Vol. 3, pp. 10–31, 2000.

45. Zoellner, J. A., "Frequency Assignment Games and Strategies", *IEEE Transac-*

tions on Electromagnetic Compatibility, Vol. 15, pp. 191–196, 1973.

46. Waldrop, J., D. Engels and S. Sarma, "Colorwave: an anticollision algorithm for the reader collision problem", *IEEE International Conference on Communications(ICC)*, Vol. 2, pp. 1206–1210, 2003.

47. Waldrop, J., D. Engels and S. Sarma, "Colorwave: a MAC for RFID reader networks", *IEEE Wireless Communications and Networking Conference*, pp. 1701–1704, 2003.

48. Kunz, D., "Channel assignment for cellular radio using neural networks", *IEEE Transactions on Vehicular Technology*, Vol. 40, pp. 188–193, 1991.

49. Kunz, D., "Channel assignment for cellular radio using simulated annealing", *IEEE Transactions on Vehicular Technology*, Vol. 42, pp. 14–21, 1993.

50. Vogt, H., "Multiple object identification with passive RFID tags", *IEEE International Conference on Systems, Man and Cybernetics*, Vol. 3, pp. 6–9, 2002.

51. Vogt, H., "Efficient object identification with passive RFID tags", *Proceedings International Conference on Pervasive Computing*, pp. 98–113, 2002.

52. Tang, Z. and Y. He, "Research of Multi-access and Anti-collision Protocols in RFID Systems", *IEEE International Workshop on Anti-counterfeiting, Security, Identification*, pp. 377–380, 2007.

53. Klair, D. K., K.-W. Chin and R. Raad, "A Survey and Tutorial of RFID Anti-Collision Protocols", *IEEE Communications Surveys & Tutorials*, Vol. 12, pp. 400–421, 2010.

54. Klair, D. K., K.-W. Chin and R. Raad, "An Investigation into thie Energy Eficiency of Pure and Slotted Aloha Based RFID Anti-Collision Protocols", *IEEE International Symposium on a World of Wireless, Mobile and Multimedia Net-*

works, pp. 1–4, 2007.

55. Zhen, B., M. Kobayashi and M. Shimizu, "Framed Aloha for multiple RFID objects identification", *IEICE-Transactions on Communications*, Vol. E88-B, pp. 991–999, 2005.

56. Cha, J.-R. and J.-H. Kim, "Novel anti-collision algorithms for fast object identification in RFID system", *The 11th Intl. Conference on Parallel and Distributed Systems*, pp. 63–67, 2005.

57. Chen, Y.-H., S.-J. Horng, R.-S. Run, J.-L. Lai, R.-J. Chen, W.-C. Chen, Y. Pan and T. Takao, "A Novel Anti-Collision Algorithm in RFID Systems for Identifying Passive Tags", *IEEE Transactions on Industrial Informatics*, Vol. 6, pp. 105–121, 2010.

58. Porta, T. F. L., G. Maselli and C. Petrioli, "Anticollision Protocols for Single-Reader RFID Systems: Temporal Analysis and Optimization", *IEEE Transactions on Mobile Computing*, Vol. 10, pp. 267–279, 2011.

59. Mays, W. M. and B. D. Moore, *RFID transponder having active backscatter amplifier for re-transmitting a received signal*, United States Patent, US 6,838,989 B1, 2005.

60. Vullers, R. J., R. van Schaijk, H. J. Visser, J. Penders and C. V. Hoof, "Energy Harvesting for Autonomous Wireless Sensor Networks", *IEEE Solid-State Circuits Magazine*, Vol. 2, pp. 29–38, 2010.

61. Jabbar, H., Y. S. Song and T. T. Jeong, "RF energy harvesting system and circuits for charging of mobile devices", *IEEE Transactions on Consumer Electronics*, Vol. 56, pp. 247–253, 2010.

62. Sample, A. and J. R. Smith, "Experimental results with two wireless power transfer systems", *IEEE Radio and Wireless Symposium*, pp. 16–18, 2009.

63. Vullers, R. J. M., H. J. Visser, B. O. het Veld and V. Pop, "RF harvesting using antenna structures on foil", *Proc. PowerMEMS*, pp. 209–212, 2008.

64. Ungan, T. and L. M. Reindl, "Harvesting low ambient RF-sources for autonomous measurement systems", *IEEE Proc. Instrumentation and Measurement Technology Conference*, pp. 62–65, 2008.

65. Liu, H.-C., M.-C. Hua, C.-G. Peng and J.-P. Ciou, "A Novel Battery-Assisted Class-1 Generation-2 RF Identification Tag Design", *IEEE Transactions on Microwave Theory and Techniques*, Vol. 57, pp. 1388–1397, 2009.

66. Janek, A., C. Trummer, C. Steger, R. Weiss, J. Preishuber-Pfluegl and M. Pistauer, "Lifecycle Extension of Long Range UHF RFID Tags based on Energy Harvesting", *The First International EURASIP Workshop on RFID Technology*, pp. 1–7, 2007.

67. Lei, J., R. Yates and L. Greenstein, "A generic model for optimizing single-hop transmission policy of replenishable sensors", *IEEE Transactions on Wireless Communications*, Vol. 8, pp. 547–551, 2009.

68. Sample, A. P., D. J. Yeager, P. S. Powledge, A. V. Mamishev and J. R. Smith, "Design of an RFID-Based Battery-Free Programmable Sensing Platform", *IEEE Transactions on Instrumentation and Measurement*, Vol. 57, pp. 2608–2615, 2008.

69. Janek, A., C. Trummer, C. Steger, R. Weiss, J. Preishuber-Pfluegl and M. Pistauer, "Simulation based verification of energy storage architectures for higher class tags supported by energy harvesting devices", *10th Euromicro Conference on Digital System Design Architectures, Methods and Tools*, pp. 462–463, 2007.

70. EPCglobal, "EPC radio-frequency identity protocols class-1 generation2 UHF RFID protocol for communications at 860 MHz - 960 MHz version 1.0.9", *EPCglobal Standard Specification*, 2004.

71. Smith, P. H., "Transmission line calculator", *Electronics*, Vol. 12, p. 29–31, 1939.

72. Malherbe, J., "The Locus of Points of Constant VSWR When Renormalized to a Different Characteristic Impedance", *IEEE Transactions on Microwave Theory and Techniques*, Vol. 25, p. 444–445, 1977.

73. Kurokawa, K., "Power Waves and the Scattering Matrix", *IEEE Transactions on Microwave Theory and Techniques*, Vol. 13, p. 194–202, 1965.

74. Nikitin, P., K. Rao, S. Lam, V. Pillai, R. Martinez and H. Heinrich, "Power Reflection Coefficient Analysis for Complex Impedances in RFID Tag Design", *IEEE Transactions on Microwave Theory and Techniques*, Vol. 53, pp. 2721–2725, 2005.

75. W.C.Jakes, *Microwave Mobile Communications*, John Wiley & Sons, Inc., New York, 1974, reprinted by IEEE Press in 1994.

76. Lee, W. C. Y., *Mobile Cellular Telecommunications: Analog and Digital Systems*, McGraw-Hill Professional, New York, 1995.

77. Rappaport, T. S., *Wireless Communications: Principles and Practice*, Prentice Hall, New Jersey, 2002.

78. Janaswamy, R., *Radiowave Propagation and Smart Antennas for Wireless Communications*, Kluwer Academic Publishers, Norwell, MA, 2001.

79. Bertoni, H., W. Honcharenko, L. R. Macel and H. Xia, "UHF propagation prediction for wireless personal communications", *Proceedings of the IEEE*, Vol. 82, pp. 1333–1359, 1994.

80. Nikitin, P. V., K. V. S. Rao and R. D. Martinez, "Differential RCS of RFID tag", *Inst.Elect.Eng.Electron.Lett.*, Vol. 43, pp. 431–432, 2007.

81. Lazaro, A., D. Girbau and D. Salinas, "Radio Link Budgets for UHF RFID

on Multipath Environments", *IEEE Transactions on Antennas and Propagation*, Vol. 57, pp. 1241–1251, 2009.

82. Xia, H., H. Bertoni, L. Maciel, A. Lindsay-Stewart and R. Rowe, "Radio propagation characteristics for line-of-sight microcellular and personal communications", *IEEE Transactions on Antennas and Propagation*, Vol. 41, pp. 1439–1447, 1993.

83. Yen, C.-C., A. E. Gutierrez, D. Veeramani and D. van der Weide, "Radar Cross-Section Analysis of Backscattering RFID Tags", *IEEE Antennas and Wireless Propagation Letters*, Vol. 6, pp. 279–281, 2007.

84. Goldsmith, A., *Wireless Communications*, Cambridge University Press, New York, 2005.

85. Kim, D., M. Ingram and W. Smith, "Measurements of small-scale fading and path loss for long range RF tags", *IEEE Transactions on Antennas and Propagation*, Vol. 51, pp. 1740–1749, 2003.

86. Penttila, K., L. Sydanheimo and M. Kivikoski, "Implementation of Tx/Rx isolation in an RFID reader", *International Journal of RFID Technology and Applications*, Vol. 1, pp. 74–89, 2006.

87. Polivka, J., "Wideband UHF/microwave active isolators", *International Journal of RFID Technology and Applications*, Vol. 1, pp. 70–72, 2006.

88. Jung, J.-W., K.-K. Nae, J. P. Thakur, H.-G. Cho, and J.-S. Park, "Directional coupler for UHF mobile RFID reader", *Microwave and Optical Technology Letters*, Vol. 49, pp. 1501–1504, 2007.

89. Son, H.-W., J.-N. Lee, and G.-Y. Choi, "Design of compact RFID reader antenna with high transmit/receive isolation", *Microwave and Optical Technology Letters*, Vol. 48, pp. 2478–2481, 2006.

90. kyu Kim, W., M. que Lee, J. hyun Kim, H. sun Lim, J. won Yu, B. jun Jang and J. seok Park, "A Passive Circulator with High Isolation using a Directional Coupler for RFID", *IEEE MTT-S International Microwave Symposium Digest*, pp. 1177–1180, 2006.

91. Griffin, J. D. and G. D. Durgin, "Gains For RF Tags Using Multiple Antennas", *IEEE Transactions on Antennas and Propagation*, Vol. 56, pp. 563–570, 2008.

92. He, C., X. Chen, Z. J. Wang and W. Su, "On the performance of MIMO RFID backscattering channels", *EURASIP Journal on Wireless Communications and Networking*, Vol. 2012, pp. 1–15, 2012.

93. Chizhik, D., G. Foschini, M. Gans and R. Valenzuela, "Keyholes, correlations, and capacities of multielement transmit and receive antennas", *IEEE Transactions on Wireless Communications*, Vol. 1, pp. 361–368, 2002.

94. Mi, M., M. H. Mickle, C. Capelli and H. Swift, "RF energy harvesting with multiple antennas in the same space", *IEEE Antennas and Propagation Magazine*, Vol. 47, pp. 100–106, 2005.

95. Patel, C., G. Stuber and T. Pratt, "Statistical properties of amplify and forward relay fading channels", *IEEE Transactions on Vehicular Technology*, Vol. 55, pp. 1–9, 2006.

96. Griffin, J. D. and G. D. Durgin, "Multipath fading measurements for multi-antenna backscatter RFID at 5.8 GHz", *IEEE International Conference on RFID*, pp. 322–329, 2009.

97. Ozel, O., K. Tutuncuoglu, J. Yang, S. Ulukus and A. Yener, "Transmission with Energy Harvesting Nodes in Fading Wireless Channels: Optimal Policies", *IEEE Journal on Selected Areas in Communications*, Vol. 29, pp. 1732–1743, 2011.

98. Devillers, B. and D. Gündüz, "Energy harvesting communication system with

battery constraint and leakage", *IEEE GLOBECOM Workshops (GC Wkshps)*, pp. 383–388, 2011.

99. Orhan, O., D. Gündüz and E. Erkip, "Throughput maximization for an energy harvesting communication system with processing cost", *IEEE Information Theory Workshop*, pp. 84–88, 2012.

100. Ho, C. K. and R. Zhang, "Optimal Energy Allocation for Wireless Communications With Energy Harvesting Constraints", *IEEE Transactions on Signal Processing*, Vol. 60, pp. 4808–4818, 2012.

101. Ozel, O. and S. Ulukus, "Information-theoretic analysis of an energy harvesting communication system", *IEEE 21st International Symposium on Personal, Indoor and Mobile Radio Communications Workshops*, pp. 330–335, 2010.

102. Boyd, S. and L. Vandenberghe, *Convex Optimization*, Cambridge University Press, New York, 2004.

103. Stewart, J., *Calculus: Early Transcendentals*, Brooks-Cole Publishing, 2016.

104. Grant, M. and S. Boyd, *CVX: Matlab Software for Disciplined Convex Programming, version 2.1*, 2014, `http://cvxr.com/cvx`, accessed at June 2018.

APPENDIX A: HARVESTED ENERGY IN AN IDLE TIME SLOT

$$E_{\text{harvest}}(t_k) = \int_{t_k}^{t_{k+1}} |y(t_k)|^2 dt = \int_{t_k}^{t_{k+1}} \left| \sqrt{P_{\text{RX,tag}}} h_{\text{dl}}(t_k) x(t_k) + n_{\text{tag}}(t) \right|^2 dt$$
$$= \int_{t_k}^{t_{k+1}} \left| \sqrt{P_{\text{TX,reader}} G_{\text{reader}} G_{\text{tag}} \left(\frac{\lambda}{4\pi d} \right)^2} h_{\text{dl}}(t_k) x(t_k) + n_{\text{tag}}(t) \right|^2 dt \quad . \tag{A.1}$$

$$E_{\text{harvest}}(t_k) = \int_{t_k}^{t_{k+1}} \left| \sqrt{P_{\text{TX,reader}} G_{\text{reader}} G_{\text{tag}} \left(\frac{\lambda}{4\pi d} \right)^2} h_{\text{dl}}(t_k) x(t_k) \right|^2 dt$$
$$+ \int_{t_k}^{t_{k+1}} \left| 2 \cdot \sqrt{P_{\text{TX,reader}} G_{\text{reader}} G_{\text{tag}} \left(\frac{\lambda}{4\pi d} \right)^2} h_{\text{dl}}(t_k) x(t_k) n_{\text{tag}}(t) \right| dt \tag{A.2}$$
$$+ \int_{t_k}^{t_{k+1}} \left| n_{\text{tag}}(t) \right|^2 dt \quad .$$

Because the transmitted signal from the reader, i.e. $x(t_k)$ and the AWGN of the tag, i.e. $n_{\text{tag}}(t)$ are independent, equation (A.1) can be written as

$$E_{\text{harvest}}(t_k) = P_{\text{TX,reader}} G_{\text{reader}} G_{\text{tag}} \left(\frac{\lambda}{4\pi d} \right)^2 |h_{\text{dl}}(t_k)|^2 \int_{t_k}^{t_{k+1}} |x(t_k)|^2 dt + 0 + T\sigma_t^2 \tag{A.3}$$

where the second term in equation (A.2)

$$= \int_{t_k}^{t_{k+1}} \left| 2 \cdot \sqrt{P_{\text{TX,reader}} G_{\text{reader}} G_{\text{tag}} \left(\frac{\lambda}{4\pi d} \right)^2} h_{\text{dl}}(t_k) x(t_k) n_{\text{tag}}(t) \right| dt$$
$$= 2 \cdot \sqrt{P_{\text{TX,reader}} G_{\text{reader}} G_{\text{tag}} \left(\frac{\lambda}{4\pi d} \right)^2} |h_{\text{dl}}(t_k)| \int_{t_k}^{t_{k+1}} \left| x(t_k) n_{\text{tag}}(t) \right| dt \tag{A.4}$$
$$= 0 \quad .$$

Due to the following equation

$$\int_{t_k}^{t_{k+1}} |x(t_k)|^2 dt = \int_{t_k}^{t_{k+1}} \left|\sqrt{2}\cos(2\pi f_0 t)\right|^2 dt = T \quad , \tag{A.5}$$

the harvested energy in idle time slots can be calculated as

$$E_{\text{harvest}}(t_k) = TP_{\text{TX,reader}}G_{\text{reader}}G_{\text{tag}}\left(\frac{\lambda}{4\pi d}\right)^2 |h_{\text{dl}}(t_k)|^2 + T\sigma_t^2 \quad . \tag{A.6}$$

APPENDIX B: SIGNAL SNR IN CASE OF PASSIVE RFID TAG

The envelope of the received signal by the reader in the conventional passive RFID system signal is

$$|z_{\text{passive}}(t_k)| = \left| \sqrt{P_{\text{TX,reader}} G_{\text{reader}}^2 G_{\text{tag}}^2 \left(\frac{\lambda}{4\pi d}\right)^4} h_{\text{dl}}(t_k) h_{\text{ul}}(t_k) x(t_k) + n_{\text{reader}}(t) \right| \quad . \tag{B.1}$$

Because the UL and DL Rayleigh fading coefficients are constant between two consecutive time slots and they are statistically independent, received signal power caused by backscatter modulated signal is denoted by

$$\begin{aligned} &\int_{t_k}^{t_{k+1}} \left| \sqrt{P_{\text{TX,reader}} G_{\text{reader}}^2 G_{\text{tag}}^2 \left(\frac{\lambda}{4\pi d}\right)^4} h_{\text{dl}}(t_k) h_{\text{ul}}(t_k) x(t_k) \right|^2 dt \\ &= P_{\text{TX,reader}} G_{\text{reader}}^2 G_{\text{tag}}^2 \left(\frac{\lambda}{4\pi d}\right)^4 |h_{\text{dl}}(t_k)|^2 |h_{\text{ul}}(t_k)|^2 \int_{t_k}^{t_{k+1}} |x(t_k)|^2 dt \\ &= T P_{\text{TX,reader}} G_{\text{reader}}^2 G_{\text{tag}}^2 \left(\frac{\lambda}{4\pi d}\right)^4 |h_{\text{dl}}(t_k)|^2 |h_{\text{ul}}(t_k)|^2 \quad . \end{aligned} \tag{B.2}$$

Hence the noise power equals to $T\sigma_t^2$, the received signal SNR in conventional passive RFID system is expressed as

$$\begin{aligned} \gamma_{\text{RX,reader,passive}}(t_k) &= \frac{T P_{\text{TX,reader}} G_{\text{reader}}^2 G_{\text{tag}}^2}{T\sigma_r^2} \left(\frac{\lambda}{4\pi d}\right)^4 |h_{\text{dl}}(t_k)|^2 |h_{\text{ul}}(t_k)|^2 \\ &= \frac{P_{\text{TX,reader}} G_{\text{reader}}^2 G_{\text{tag}}^2}{\sigma_r^2} \left(\frac{\lambda}{4\pi d}\right)^4 |h_{\text{dl}}(t_k)|^2 |h_{\text{ul}}(t_k)|^2 \quad . \end{aligned} \tag{B.3}$$

APPENDIX C: SIGNAL SNR IN CASE OF ABEH RFID TAG

The envelope of the received signal by the reader coming from the ABEH tag is defined as

$$|z_{\text{enhanced}}(t_k)| = \left| \sqrt{P_{\text{RX,reader}}|h_{\text{dl}}(t_k)|^2 + P_{\text{amp},k}G_{\text{reader}}G_{\text{tag}}\left(\frac{\lambda}{4\pi d}\right)^2} h_{\text{ul}}(t_k)x(t_k) + n_{\text{reader}}(t) \right| . \tag{C.1}$$

Since the UL and DL Rayleigh fading coefficients are constant between two consecutive time slots and they are statistically independent, received signal power caused by ABEH tag is

$$\begin{aligned}
&\int_{t_k}^{t_{k+1}} \left| \sqrt{P_{\text{RX,reader}}|h_{\text{dl}}(t_k)|^2 + P_{\text{amp},k}G_{\text{reader}}G_{\text{tag}}\left(\frac{\lambda}{4\pi d}\right)^2} h_{\text{ul}}(t_k)x(t_k) \right|^2 dt \\
&= P_{\text{TX,reader}}G_{\text{reader}}^2G_{\text{tag}}^2\left(\frac{\lambda}{4\pi d}\right)^4 |h_{\text{dl}}(t_k)|^2|h_{\text{ul}}(t_k)|^2 \int_{t_k}^{t_{k+1}} |x(t_k)|^2 dt \\
&+ P_{\text{amp},k}G_{\text{reader}}G_{\text{tag}}\left(\frac{\lambda}{4\pi d}\right)^2 |h_{\text{ul}}(t_k)|^2 \int_{t_k}^{t_{k+1}} |x(t_k)|^2 dt \\
&= TP_{\text{TX,reader}}G_{\text{reader}}^2G_{\text{tag}}^2\left(\frac{\lambda}{4\pi d}\right)^4 |h_{\text{dl}}(t_k)|^2|h_{\text{ul}}(t_k)|^2 \\
&+ TP_{\text{amp},k}G_{\text{reader}}G_{\text{tag}}\left(\frac{\lambda}{4\pi d}\right)^2 |h_{\text{ul}}(t_k)|^2 \quad .
\end{aligned} \tag{C.2}$$

Hence the noise power equals to $T\sigma_r^2$, the received signal SNR in conventional passive RFID system is given by

$$\begin{aligned}
\gamma_{\text{RX,reader,ABEH}}(t_k) = &\frac{TP_{\text{TX,reader}}G_{\text{reader}}^2G_{\text{tag}}^2}{T\sigma_r^2}\left(\frac{\lambda}{4\pi d}\right)^4 |h_{\text{dl}}(t_k)|^2|h_{\text{ul}}(t_k)|^2 \\
&+ \frac{TP_{\text{amp},k}G_{\text{reader}}G_{\text{tag}}}{T\sigma_r^2}\left(\frac{\lambda}{4\pi d}\right)^2 |h_{\text{ul}}(t_k)|^2 \quad .
\end{aligned} \tag{C.3}$$

$$\gamma_{\mathrm{RX,reader,ABEH}}(t_k) = \frac{P_{\mathrm{TX,reader}} G_{\mathrm{reader}}^2 G_{\mathrm{tag}}^2}{\sigma_r^2} \left(\frac{\lambda}{4\pi d}\right)^4 |h_{\mathrm{dl}}(t_k)|^2 |h_{\mathrm{ul}}(t_k)|^2 + \frac{P_{\mathrm{amp},k} G_{\mathrm{reader}} G_{\mathrm{tag}}}{\sigma_r^2} \left(\frac{\lambda}{4\pi d}\right)^2 |h_{\mathrm{ul}}(t_k)|^2 \quad . \tag{C.4}$$

APPENDIX D: READ PROBABILITY UNDER RAYLEIGH CHANNEL

Received signal SNR in ABEH scenario is given by

$$\gamma_{\mathrm{RX,reader,ABEH}}(t_k) = \frac{P_{\mathrm{TX,reader}} G_{\mathrm{reader}}^2 G_{\mathrm{tag}}^2}{\sigma_r^2} \left(\frac{\lambda}{4\pi d}\right)^4 |h_{\mathrm{dl}}(t_k)|^2 |h_{\mathrm{ul}}(t_k)|^2 \eta_{\mathrm{mod}} + \frac{P_{\mathrm{amp},k} G_{\mathrm{reader}} G_{\mathrm{tag}}}{\sigma_r^2} \left(\frac{\lambda}{4\pi d}\right)^2 |h_{\mathrm{ul}}(t_k)|^2 \eta_{\mathrm{amp}} \quad . \tag{D.1}$$

Suppose that $X = |h_{\mathrm{dl}}(t_k)|^2$, $Y = |h_{\mathrm{ul}}(t_k)|^2$, $K = \gamma_{\mathrm{RX,reader,ABEH}}(t_k)$,

$a = \frac{P_{\mathrm{TX,reader}} G_{\mathrm{reader}}^2 G_{\mathrm{tag}}^2}{\sigma_r^2} \left(\frac{\lambda}{4\pi d}\right)^4 \eta_{\mathrm{mod}}$ and $b = \frac{P_{\mathrm{amp},k} G_{\mathrm{reader}} G_{\mathrm{tag}}}{\sigma_r^2} \left(\frac{\lambda}{4\pi d}\right)^2 \eta_{\mathrm{amp}}$. Since $|h_{\mathrm{ul}}(t_k)|$ and $|h_{\mathrm{dl}}(t_k)|$ are Rayleigh distributed random variables, $|h_{\mathrm{ul}}(t_k)|^2$ and $|h_{\mathrm{dl}}(t_k)|^2$ are exponentially distributed random variables which is proven in Appendix E. Therefore X and Y are also exponentially distributed random variables. So $K = aXY + bY$ is also random variable which implies the received signal SNR. Thus the read probability can be written as

$$Pr[\gamma_{\mathrm{RX,reader,ABEH}}(t_k) \geq \gamma_{\mathrm{th,reader}}] = Pr[K \geq \gamma_{\mathrm{th,reader}}] = 1 - \int_0^{\gamma_{\mathrm{th,reader}}} f_K(k) dk \quad . \tag{D.2}$$

Let $f_K(k) = \int_{-\infty}^{\infty} f_K(k|x = \beta) f_X(\beta) d\beta$ where β is dummy variable and $\beta \geq 0$ because X is exponentially distributed. Since $K = aXY + bY = a\beta Y + bY = (a\beta + b)Y$. Thus

$$
\begin{aligned}
1-\int_0^{\gamma_{\text{th,reader}}} f_K(k)dk &= 1-\int_0^{\gamma_{\text{th,reader}}}\int_0^{\infty} f_K(k|x=\beta)f_X(\beta)d\beta dk \\
&= 1-\left[\int_0^{\infty} f_X(\beta)d\beta\right]\left[\int_0^{\gamma_{\text{th,reader}}} \frac{1}{|a\beta+b|} f_Y\left(\frac{k}{a\beta+b}\right)dk\right] \\
&= 1-\left[\int_0^{\infty} e^{-\beta}d\beta\right]\left[\int_0^{\gamma_{\text{th,reader}}} \frac{1}{a\beta+b} e^{-\left(\frac{k}{a\beta+b}\right)}dk\right] \\
&= 1-\left[\int_0^{\infty} e^{-\beta}\left(1-e^{-\frac{\gamma_{\text{th,reader}}}{a\beta+b}}\right)d\beta\right] \\
&= 1-\left[1-\int_0^{\infty} e^{-\frac{\gamma_{\text{th,reader}}}{a\beta+b}-\beta}d\beta\right] \\
&= \int_0^{\infty} e^{-\frac{\gamma_{\text{th,reader}}}{\text{a}\beta+\text{b}}-\beta}d\beta \quad .
\end{aligned}
\tag{D.3}
$$

by replacing back dummy variable β with y, a=$\frac{P_{\text{TX,reader}}G_{\text{reader}}^2 G_{\text{tag}}^2}{\sigma_r^2}\left(\frac{\lambda}{4\pi d}\right)^4\eta_{\text{mod}}$ and b with $\frac{P_{\text{amp},k}G_{\text{reader}}G_{\text{tag}}}{\sigma_r^2}\left(\frac{\lambda}{4\pi d}\right)^2\eta_{\text{amp}}$ yields the following:

$$
\begin{aligned}
\overline{p}_{\text{read}} &= \frac{1}{N}\sum_{k=1}^{N} Pr[\gamma_{\text{RX,reader,ABEH}}(t_k) \geq \gamma_{\text{th,reader}}] \\
&= \frac{1}{N}\sum_{k=1}^{N}\int_0^{\infty} e\left[-\frac{\gamma_{\text{th,reader}}\sigma_r^2}{P_{\text{TX,reader}}G_{\text{reader}}^2 G_{\text{tag}}^2\left(\frac{\lambda}{4\pi d}\right)^4\eta_{\text{mod}}y + P_{\text{amp},k}G_{\text{reader}}G_{\text{tag}}\left(\frac{\lambda}{4\pi d}\right)^2\eta_{\text{amp}}} - y\right]dy \quad .
\end{aligned}
\tag{D.4}
$$

APPENDIX E: POWER PROFILE OF RAYLEIGH DISTRIBUTION

Let $Z_1, Z_2 \sim \mathcal{N}(0,1)$ where 1 is the variance of the normal distributed random variables. Since $|h_{\text{dl}}|$ is Rayleigh distributed, $h_{\text{dl}} = \frac{1}{\sqrt{2}}(Z_1 + jZ_2)$. Let

$$M = |h_{\text{dl}}| = \frac{1}{\sqrt{2}} \cdot \sqrt{Z_1^2 + Z_2^2} \tag{E.1}$$

where M is also Rayleigh distributed random variable, i.e. $M \sim Rayleigh(\sigma_m = \frac{1}{\sqrt{2}})$ where the probability distribution function (pdf) of a Rayleigh distributed random variable is expressed as

$$f_M(m) = \frac{m}{\sigma_m^2} e^{-\left(\frac{m^2}{2\sigma_m^2}\right)} = 2me^{-m^2}, m \geq 0 \ . \tag{E.2}$$

Suppose that $X = M^2 = |h_{\text{dl}}|^2$ which is also random variable. Thus the cumulative distribution function(cdf) of X is

$$\begin{aligned} F_X(x) = \text{Prob}[X \leq x] = \text{Prob}[M^2 \leq x] = \text{Prob}[M \leq \sqrt{x}] = \int_0^{\sqrt{x}} f_M(m)dm \\ = \int_0^{\sqrt{x}} 2me^{-m^2}dm = \int_0^x e^{-u}du = [1 - e^{-x}] \ . \end{aligned} \tag{E.3}$$

Thus, the pdf of $X = M^2 = |h_{\text{dl}}|^2$ is calculated as

$$f_X(x) = \frac{F_X(x)}{dx} = \frac{[1 - e^{-}x]}{dx} = e^{-x}, x \geq 0 \ . \tag{E.4}$$

Therefore, $X = M^2 = |h_{\text{dl}}|^2$ is an exponential random variable, i.e. $X = |h_{\text{dl}}|^2 \sim \text{Exp}(\lambda_x = 1)$.

APPENDIX F: READ PROBABILITY IN DELAY-CONSTRAINED MODEL

Since harvested energy values should be priorly known for off-line policy, $|h_{\mathrm{dl}}(t_{i_k})|^2$ cannot be thought as random anymore. Assume that $\mathrm{K} = P_{\mathrm{RX,reader,ABEH}}(t_{i_k})$, $Y = |h_{\mathrm{ul}}(t_{i_k})|^2$, $a = P_{\mathrm{TX,reader}}|h_{\mathrm{dl}}(t_{i_k})|^2\left(\frac{\lambda}{4\pi d}\right)^4\eta_{\mathrm{mod}}$, $b_k = P_{\mathrm{amp},i_k}\left(\frac{\lambda}{4\pi d}\right)^2\eta_{\mathrm{amp}}$. Thus, $K = aY + bY = (a+b)Y$ is also random variable. Read probability for off-line energy harvesting policy can be defined as

$$Pr(P_{\mathrm{RX,reader}}(t_{i_k}) \geq P_{\mathrm{th,reader}}) = Pr(K \geq P_{\mathrm{th,reader}}) \quad . \tag{F.1}$$

If $Y = cX$ then $f_Y(y) = \frac{1}{|c|}f_X(\frac{y}{c})$ where X and Y are random variables and c is constant. Thus $f_K(k) = \frac{1}{|a+b|}f_Y(\frac{k}{a+b})$. Note that Y has exponential distribution.Thus

$$\begin{aligned} Pr(K \geq P_{\mathrm{th,reader}}) &= 1 - \left[\int_0^{P_{\mathrm{th,reader}}} \frac{1}{|a+b|}f_Y(\frac{k}{a+b})dk\right] \\ &= 1 - \frac{1}{|a+b|}\left[\int_0^{P_{\mathrm{th,reader}}} \left(e^{-\frac{k}{a+b}}\right)dk\right] = e^{-\frac{P_{\mathrm{th,reader}}}{a+b}} \end{aligned} \tag{F.2}$$

or by replacing $a = P_{\mathrm{TX,reader}}|h_{\mathrm{dl}}(t_{i_k})|^2(\frac{\lambda}{4\pi d})^4\eta_{\mathrm{mod}}$ and $b_k = P_{\mathrm{amp},i_k}(\frac{\lambda}{4\pi d})^2\eta_{\mathrm{amp}}$, the objective function for off-line energy harvesting power policy is

$$\Pr(P_{\mathrm{RX,reader}}(t_{i_k}) \geq P_{\mathrm{th,reader}}) = e^{-\frac{P_{\mathrm{th,reader}}}{P_{\mathrm{TX,reader}}|h_{\mathrm{dl}}(t_{i_k})|^2(\frac{\lambda}{4\pi d})^4\eta_{\mathrm{mod}} + P_{\mathrm{amp},i_k}(\frac{\lambda}{4\pi d})^2\eta_{\mathrm{amp}}}} \quad . \tag{F.3}$$

APPENDIX G: READ PROBABILITY IN DELAY-TOLERANT MODEL

The read probability with SC assumption in delay-tolerant model is

$$\begin{aligned}\overline{p}_{\text{read}} &= \frac{1}{N}\sum_{k=1}^{N}\Pr\left[\max\left(\gamma_{\text{RX,reader}}(t_{i_k}),...,\gamma_{\text{RX,reader}}(t_{i_k+M})\right)\geq\gamma_{\text{th,reader}}\right],\\ &= \frac{1}{N}\sum_{k=1}^{N}\left(1-\Pr\left[\max\left(\gamma_{\text{RX,reader}}(t_{i_k}),...,\gamma_{\text{RX,reader}}(t_{i_k+M})\right)\leq\gamma_{\text{th,reader}}\right]\right),\\ &= \frac{1}{N}\sum_{k=1}^{N}\left(1-\prod_{u=0}^{M}\Pr\left(\gamma_{\text{RX,reader}}(t_{i_k+u})\leq\gamma_{\text{th,reader}}\right)\right).\end{aligned} \tag{G.1}$$

Since

$$\Pr\left(\gamma_{\text{RX,reader}}(t_{i_k+u})\leq\gamma_{\text{th,reader}}\right)=1-\exp\left(-\frac{\gamma_{\text{th,reader}}}{\gamma_{\text{TX,reader}}|h_{dl}(t_{i_k+u})|^2\left(\frac{\lambda}{4\pi d}\right)^4\eta_{\text{mod}}+\gamma_{\text{amp,i}_\text{k}+\text{u}}\left(\frac{\lambda}{4\pi d}\right)^2\eta_{\text{amp}}}\right),$$

then

$$\overline{p}_{\text{read}}=\tfrac{1}{N}\sum_{k=1}^{N}\left[1-\prod_{u=0}^{M}\left[1-\exp\Big(-\frac{\gamma_{\text{th,reader}}}{\gamma_{\text{TX,reader}}|h_{dl}(t_{i_k+u})|^2\left(\frac{\lambda}{4\pi d}\right)^4\eta_{\text{mod}}+\gamma_{\text{amp,i}_\text{k}+\text{u}}\left(\frac{\lambda}{4\pi d}\right)^2\eta_{\text{amp}}}\Big)\right]\right].$$

Equivalently,

$$\overline{p}_{\text{read}}=1-\tfrac{1}{N}\sum_{k=1}^{N}\left[\prod_{u=0}^{M}\left[1-\exp\Big(-\frac{\gamma_{\text{th,reader}}}{\gamma_{\text{TX,reader}}|h_{dl}(t_{i_k+u})|^2\left(\frac{\lambda}{4\pi d}\right)^4\eta_{\text{mod}}+\gamma_{\text{amp,i}_\text{k}+\text{u}}\left(\frac{\lambda}{4\pi d}\right)^2\eta_{\text{amp}}}\Big)\right]\right].$$

Let's define $a=\gamma_{\text{th,reader}}$, $b_{k,u}=\gamma_{\text{TX,reader}}|h_{dl}(t_{i_k+u})|^2\left(\frac{\lambda}{4\pi d}\right)^4\eta_{\text{mod}}$, $g=\left(\frac{\lambda}{4\pi d}\right)^2\eta_{\text{amp}}$ and $x_{k,u}=\gamma_{\text{amp,i}_\text{k}+\text{u}}$. Therefore the average read probability of the SC-based delay-

tolerant model is

$$\overline{p}_{\text{read}} = 1 - \frac{1}{N}\sum_{k=1}^{N}\left[\prod_{u=0}^{M}\left[1 - \exp\Big(-\frac{a}{b_{k,u} + g x_{k,u}}\Big)\right]\right]. \tag{G.2}$$